Supporting Information for

Is a small singlet-triplet energy gap a guarantee for TADF performance in MR-TADF compounds? Impact of the triplet manifold energy splitting

Rasa Keruckiene[a], Aliaksei A. Vaitusionak[b], Maksim I. Hulnik[b], Ivan A. Berezianko[b], Dalius Gudeika[a], Simas Macionis [a], Malek Mahmoudi[a], Dmytro Volyniuk[a], DanilloValverde [c], Yoann Olivier[c*], Kai Lin Woon[d], Sergei V Kostjuk[b,e], Sebastian Reineke[f], Juozas V. Grazulevicius[a*], Gjergji Sini [g*]

[a] Department of Polymer Chemistry and Technology, Kaunas University of Technology, K. Barsausko st. 59, LT-50254, Kaunas, Lithuania

[b] Research Institute for Physical Chemical Problems of the Belarusian State University, 14, Leningradskaya st, 220030 Minsk, Belarus

[c]Laboratory for Computational Modeling of Functional Materials, Namur Institute of Structured Matter, University of Namur, Rue de Bruxelles, 61, B-5000 Namur, Belgium.

[d] Low Dimensional Material Research Centre, Department of Physics, University Malaya, Kuala Lumpur, Malaysia

[e] Department of Chemistry, Belarusian State University, Leningradskaya st. 14, 220006, Minsk, Belarus

[f] Dresden Integrated Center for Applied Physics and Photonic Materials (IAPP), Technische Universität Dresden, Dresden 01062, Germany;

[g]Laboratoire de Physicochimie des Polymères et des Interfaces, EA 2528, CY Cergy Paris Université, 5 mail Gay-Lussac, 95031 Cergy-Pontoise Cedex, France.

Contents

Instrumental

^1H (400 MHz) and ^{13}C (100 MHz) NMR spectra were recorded on a Bruker Avance III apparatus, while ^1H (500 MHz) and ^{13}C (125 MHz) NMR spectra were recorded on Bruker AC-500 spectrometers using $CDCl_3$ or DMSO-d_6 as solvents at room temperature. Mass spectra were obtained on a *Waters SQ Detector 2* mass spectrometer. The samples were prepared as diluted solutions of the compounds and were ionized by using electrospray ionization. Mass spectra are presented as an abundance of the ion versus the mass-to-charge ratio (*m/z*).

The X-ray diffraction measurements at grazing incidence (XRDGI) were performed using a D8 Discover diffractometer (Bruker) with Cu Kα (λ = 1.54 Å) X-ray source. Parallel beam geometry with 60 mm Göbel mirror (X-ray mirror on a high precision parabolic surface) was used. This configuration enables transforming the divergent incident X-ray beam from a line focus of the X-ray tube into a parallel beam that is free of Kβ radiation. The single crystal CIF fie can be found as a Supplementary Annex 1. Differential scanning calorimetry (DSC) measurements were recorded by using TA Instruments DSC Q2000 equipment under a flow of nitrogen (40 mL/min) at heating and cooling rates of 10 °C/min. Thermogravimetric analyses (TGA) were performed on TA Instruments TGA Q50 apparatus by recording the weight loss within the temperature range 20-800 °C at the rate of 20 °C/min under a nitrogen atmosphere (50 mL/min).[1]

Cyclic voltammetry (CV) measurements were performed with mAUTOLAB Type III galvanostat and a glassy carbon working electrode in a three-electrode cell. The measurements were carried out using 0.1 M tertbutyl ammonium hexafluorophosphate as an electrolyte and anhydrous dichloromethane at room temperature in a nitrogen atmosphere. The potentialswere measured against silver as a quasi-reference electrode. Platinum wire was used as a counter electrode. The potentials were calibrated with the standard ferrocene/ferrocenium (Fc/Fc+) redox system.

UV-vis spectra of dilute solutions (10^{-5} M) and solid samples were recorded using UV–VIS–NIR Avantes AvaSpec-2048XL spectrophotometer. Photoluminescence spectra, phosphorescence spectra, photoluminescence quantum yield (PLQY), and photoluminescence decay curves of both dilute solutions (10^{-5} M) and solid films were measured using Edinburgh Instruments FLS980 spectrometer at room temperature and 77 K. The solid films were prepared by spin-coating and left to dry at room temperature. Photoluminescence quantum yields of the films, and solutions were measured using FLS980 spectrometer equipped with an integrating sphere (inner diameter of 120 mm) calibrated with two

analytical standards: rhodamine 6G in ethanol and quinine sulphate in 0.1 M H_2SO_4. Edinburgh Instruments FLS980 spectrometer equipped with PicoQuant LDH-DC- 375 laser (wavelength 374 nm) as the excitation source, Oxford Instrument Optistat DN2 cryostat and turbo-molecular pump (capable of achieving 10^{-5} Torr pressure) was used for temperature-dependent experiments. Measurements at room temperature were done in the vacuum using the cryostat, while the experiments in different temperatures were done using the same cryostat under the continuous flow of liquid nitrogen.

The DG7 emitter was tested in vacuum-deposited OLEDs which were fabricated using 1″× 1″ pre-patterned 90-nm thick ITO (indium tin oxide)-coated glass substrates. ITO substrates were cleaned in an ultrasonic bath in N-methyl-2-pyrrolidon, ethanol and distilled water. Oxygen plasma treatment was used for 10 minutes to clean the dried substrates. Organic and metal layers were thermally evaporated by step-by-step depositions of different layers at rates between 0.5 to 1 Å/s in multi-chamber, UHV deposition tool with a vacuum pressure of 10-8 mbar. Thicknesses and evaporation rates of the layers were monitored using quartz crystal microbalance (QCM). The doped layers in emissive layers were prepared by co-evaporation of host and guest at the same time with corresponding rates. The fabricated devices were encapsulated immediately after the evaporation of aluminum cathodes by glass lids and epoxy resin in a nitrogen atmosphere (The glass lids included getters to absorb reactive molecules). The measurements of the encapsulated devices were carried out under an ambient atmosphere. Optical and electrical characteristics of the OLEDs were recorded using a calibrated photodiode, a source measuring unit (Keithley SMU 2400), calibrated spectrometer, and SweepMe! test and measurement software.

In the setup for the TOF measurements, EKSPLA NL300 laser (excitation wavelength of 355 nm), 6517B electrometer (Keithley), and TDS 3032C oscilloscope (Tektronix) are used. To test the ability to transport holes and electrons of compounds **1–6**, TOF transients under positive and negative polarity of applied electric fields are recorded. When two different slopes (intercepts of which give the transit times (t_{tr})) are obtained from the corresponding TOF transients build in log-log scales, hole and electron mobilities are calculated according to the equation $\mu = d^2/(U \times t_{tr})$ taking transit times t_{tr} from the photocurrent transients at applied voltage (U) and thicknesses of the layers (d) measured by the charge extraction by linearly increasing voltage (CELIV) technique assuming dielectric constant $\varepsilon = 3$ for the studied compounds. The samples for the TOF are fabricated on pre-patterned and pre-cleaned ITO glass substrates with sheet

resistance of 15 Ω/sq. The films for the TOF measurements are vacuum deposited with Kurt J. Lesker equipment integrated into glove box.

Quantum Chemical Calculations

Ground and the first excited states of **DG7** were optimized by resorting to the Density Functional Theory (DFT) and Time-Dependent (TD-)DFT formalisms using PBE0 as functional together with the 6-31G(d,p) Pople basis set. Harmonic frequency calculation on the optimized geometries revealed that all frequencies are positive, indicating that these structures correspond to a minimum of the potential energy surface (PES). Single-point vertical excitation energies calculation on top of the PBE0 optimized structures was performed using second-order approximate coupled cluster singles and doubles with the spin-component scaling correction (SCS-CC2) [2] and correlation consistent double- ζ atomic basis set (cc-pVDZ[3]). The optimization was done with Gaussian 16[4], while SCS-CC2 calculations were carried out with Turbomole 7.4[5]. The hole-hole Tamm-Dancoff-aproximated density functiona. The hole-hole Tamm-Dancoff-aproximated density functional theory (hh-tda[6]) calculations were performed using Terachem [2] 1.95 software and a Graphics Processing Unit server that had 32 GB random-access memory install to support three Tesla Titan X graphic cards.[7]

The spin orbit coupling values were calculated by means of pySOC software[8] applied on the results obtained by means of TDDFT calculations. The TDDFT calculations were performed on at the B3LYP/6-311G(d,p) level by utilizing the Gaussian16[4].

The vibronically-resolved emission spectrum was simulated at room temperature (T=300K) within the undistorted displaced harmonic oscillator (DHO) approximation, which considers identical frequencies and normal modes for the ground and excited states. Additionally, the Thermal Vibrational Correlation Function (TVCF) and Franck-Condon (FC) approaches are employed to obtain the emission cross-section in the frequency domain defined as follows [9]:

$$\sigma^{FC}(\omega) = \frac{2\omega^3}{3\pi\hbar c}|\mu_{if}| \int_{-\infty}^{\infty} \exp\left[-i(\omega - \omega_{if})\right] Z_{iv}^{-1}\rho_{if}^{FC}(t,T)dt$$

where, μ_{if} is the electronic transition dipole moment vector computed between the initial and final states on the optimized structure of the S_1 state, ω_{if} is the wave number and is inversely proportional to the

energy gap between the initial and final states, Z_{iv} is the partition function, and $\rho_{iv}^{FC}(t,T)$ is the thermal correction function that writes as:

$$\rho_{iv}^{FC}(t,T) = Tr\left[\exp\left(i\varepsilon_{f,v_f}\tau_f\right)\exp\left(i\varepsilon_{i,v_i}\tau_i\right)\right]$$

in which, ε_{i,v_i} and ε_{f,v_f} are, respectively, the vibrational energy level of the initial and final state, $\tau_f = t/\hbar$, and $\tau_i = \tau_f - (K_B T)^{-1}$. The emission spectrum was computed using MOMAP 2022a [10] with the adiabatic energy between the ground and S_1 states computed at the SCS-CC2/cc-pVDZ level.

The Huang-Rhys factor represents the projection of the geometry displacement between the electronic states i and f along the j-th normal mode and is defined as follows:

$$S_j = \frac{1}{2}\left\{\sqrt{\frac{\omega_j}{\hbar}}[X_f - X_i]M^{\frac{1}{2}}L_j(f)\right\}^2$$

in which ω_j is the vibrational frequency of the j-th normal mode, X_i and X_j are the Cartesian coordinates of the equilibrium geometry of states i and f, M is the diagonal matrix containing the atomic masses, $L_j(f)$ is the vector that includes the normal coordinates written in terms of mass weighted Cartesian coordinates of the final state. The contribution of an individual normal mode within the harmonic approximation is expressed in terms of its HR factor:

$$\lambda_{ij} = \hbar\omega_{ij}S_j$$

Molecular Dynamics Simulations

Molecular dynamic simulation was performed using GROMACS 2021.2[11]. The Temperature coupling using velocity rescaling with a stochastic term like Berendsen method was employed to maintain the temperature of the system constant, with a coupling time of 0.1 ps (NVT ensemble). The LINCS algorithm [12] was applied to constrain all the bond lengths within the system. The non-bonded interactions within a 1.4 nm cutoff were evaluated every step with particle mesh ewald (PME) for long-range Coulomb interaction. A time step of 1 fs was used to integrate the equations of motion using leap-frog [13] stochastic dynamics integrator. The simulation box of 1000 nm³ cubic volume has a periodicity in all directions. The topology that uses the GROMOS 54A7 forcefield was generated using Automated Topology Builder using the ground-state optimized structure at the b3lyp/def-2vp level of theory. In NPT ensemble, Parrinello Rahman[14] coupling time constant of 1 is used. Each MD run used 32 cores with

64G RAM. In order to ensure well mixing of emitter in Zeonex, the NVT was carried out at 600 K for 20 ns before running another 20 ns at 300 K followed by 5 ns at NPT at 300K.

Materials

5,11-dihydro-indolo[2,3-b]carbazole (Sigma Aldrich, 97%), iodobenzene (Sigma Aldrich, 98%), CuI (Sigma Aldrich, ≥99.5%), 1,10-phenanthroline (Sigma Aldrich, ≥99%), K_2CO_3 (Sigma Aldrich, ≥99%), 18-crown-6 (Sigma Aldrich, 99%), 1-bromo-2,6-difluorobenzene (Sigma Aldrich, 98%), *t*-BuOK (Sigma Aldrich, ≥98%), *n*-BuLi (1.6M in hexane, Sigma Aldrich), BBr_3 (1M in CH_2Cl_2, Sigma Aldrich) *N,N*-diisopropylethylamine (Sigma Aldrich, ≥99%) were used as received. Solvents dimethylformamide (DMF) (Sigma Aldrich, 99.8%) and *tert*-butylbenzene (Sigma Aldrich, 99%) were dried over calcined molecular sieves and stored in argon atmosphere.

5-Phenyl-5,11-dihydroindolo[2,3-b]carbazole (**dg7-2**). 5,11-dihydro-indolo[2,3-b]carbazole (3 g, 11.7 mmol), CuI (0.28 g, 1.47 mmol), 1,10-phenanthroline (0.52 g, 2.88 mmol), K_2CO_3 (0.39 g, 2.8 mmol) and 18-crown-6 (34 mg, 0.13 mmol) were dissolved in anhydrous DMF (295 mL) under Ar. Iodobenzene (1 mL, 8.9 mmol) was added to the solution and the reaction mixture was stirred at 140 °C for 20 h. When the reaction was finished (TLC control), the mixture was cooled down to the room temperature and filtered from precipitate on celite. The solvent was evaporated under the vacuum. The product was purified by silica gel column chromatography using hexane:DCM (1:2) as an eluent. Greywish solid was obtained with the yield of 38 % (1.12 g). MW = 322.4 g/mol ($C_{24}H_{16}N_2$).

MS (ES$^+$), m/z = 322.1 [M]$^+$.

^{1}H NMR (400 MHz, DMSO), δ (ppm): 7.10 (t, 1H,), 7.27 (t, 1H), 7.34-7.44 (m, 3H), 7.49 (s, 1H), 7.57 (m, 1H). 7.68-7.77 (m, 4H), 8.07 (s, 1H), 8.16 (d, 1H), 8.27 (s, 1H), 8.35 (d, 1H), 11.19 (s, 1H, NH).

^{13}C NMR (100 MHz, DMSO), δ (ppm): 99.5, 101.0, 109.1, 110.6, 117.9, 119.3, 120.4, 120.6, 122.5, 122.7, 122.8, 123.0, 125.8, 126.1, 126.8, 127.3, 130.3, 135.7, 135.8, 137.7, 141.2, 141.23.

11,11'-(2-bromo-1,3-phenylene)bis(5-phenyl-5,11-dihydroindolo[3,2-b]carbazole) (**dg7-1**). **dg7-2** (1 g, 3 mmol) and *t*-BuOK (0.37 g, 3.3 mmol) were dissolved in DMF (43 mL) at room temperature. After stirring for 30 min, 1-bromo-2,6-difluorobenzene (0.161 mL, 1.4 mmol) was added to the solution. The mixture was stirred at 100 °C for 48 h. After cooling to room temperature, the reaction mixture was poured into a large amount of water. The product was extracted with DCM, and the combined organic layer was dried over anhydrous Na_2SO_4. After filtration and evaporation, the crude product was purified

by silica gel column chromatography using hexane:DCM (3:1) as an eluent to afford **dg7-1** as a yellowish solid (yield = 0.84 g, 73%). MW = 817.8 g/mol ($C_{54}H_{33}BrN_4$).

MS (ES$^+$), m/z = 817.03 [M]$^+$.

^{1}H NMR (400 MHz, DMSO), δ (ppm): 7.15-7.65 (m, 14H,), 7.67-7.83 (m, 8H), 8.04-8.14 (m, 4H), 8.2 (d, 2H), 8.28-8.35 (m, 2H), 8.38 (s, 1H), 8.42 (d, 1H), 8.64 (d, 1H).

11-Phenyl-1-(11-phenylindolo[3,2-b]carbazol-5(11H)-yl)-11,16-dihydrobenzo[5,6][1,4]benzazaborinino[1,2,3-lm]indolo[3,2-b]carbazole **dg7**.To a solution of **dg7-1** (0.8 g, 0.98 mmol) in *tert*-butylbenzene (10 mL) was slowly added *n*-BuLi (1.6 M in hexane, 1 mL, 1.57 mmol) at 0 °C. After reacting for 4 h at room temperature, BBr$_3$ (1M in CH$_2$Cl$_2$, 1.6 mL, 1.57 mmol) was slowly added at 0°C, and then the mixture was stirred at room temperature for 12 h. After addition of NEt(*i*-Pr)$_2$ (0.45 mL, 2.58 mmol) at 0°C, the reaction mixture was further stirred at 170°C for 24 h. After cooling to room temperature, the reaction mixture was carefully quenched by addition of water. The product was extracted with dichloromethane, and the combined organic layer was dried over anhydrous Na$_2$SO$_4$. After filtration and evaporation, the crude product was purified twice by column chromatography on silica gel (eluent: hexane/DCM = 2:1, v/v) and recrystallize from chloroform/methanol to afford **dg7** as red crystals (yield = 0.21 g, 15%). M.p. = 357 °C (DSC). MW = 746.7 g/mol ($C_{54}H_{31}BN_4$).

MS (ES$^+$), m/z = 746.5 [M]$^+$.

^{1}H NMR (500 MHz, CDCl$_3$), δ (ppm): 6,90-7,16 (m, 6H), 7,54-7,79 (m, 18H), 7,98-8,26 (m, 3H), 8.29 (d, 2H), 8.55 (d, 2H).

Annex I
Oxygen impact

Figures 4e, f and **Figures S5** indicate important increase in the emission intensity after degassing (bubbling N2), with a ratio of 1.44 between degassed and in-air emission intensities, whereas the PLQY increases from 69% for the in-air solution to 83% upon degassing. Intriguingly, the air sensitivity of **DG7** in comparison to other multiple resonance type TADF material seems to be much lower, which is coherent with its very small delayed fluorescence fraction.[15] [16] This observation, indicates that in spite of the similarity of **DG7** with the well-known multi resonance TADF material such as DABNA-1, which

possesses a thermally accessible ΔE_{ST} but no TADF in toluene solution or in a solid matrix such as polystyrene. [17] still important differences remain to understand.

It is worth noting at this point that, while the oxygen impact is commonly related with the triplet- but also to singlet quenching, we suggest that the degassing procedure by means of N2 bubbling also helps a better solubilization by microaggregate destruction. Indeed, **Figures 4e, f** and **Figures S5** indicate an important increase in the emission intensity after sonication, with a cumulative effect of the sonication and of degassing being important. This observation is supported by the calculated PLQY after sonication and degassing, reaching a very high value of 100%.

Given that the triplets are absent in the case of **Figure 4f** (population of S1 only), we are led to the conclusion that the gain in intensity practically stems from the elimination of ACQ (sonication) and of the singlet quenching (O2). The gain in emission intensity after sonication and de-oxygenation are similar in the case of **Figure 4e** (population of S2). The difference in the ratios (Sonication+N2)/O2 is slightly larger for excitation at 350 nm than for 550 nm (4.6 and 3.9, respectively), suggesting minor impact of deoxygenation on the triplet quenching even in the case of excitation at 350 nm.

Annex II

Aiming at understanding observation of DF in ZEONEX and **DG7** solid mixture, we have performed classical molecular dynamics (MD) simulations by mixing **DG7** with DPEPO and with mCP. In these simulations, **DG7** molecules are embedded into the host molecules at a weight concentration of ~ 8%. Using Gromos54A7 forcefield, following NVT and NPT equilibration, the configurations of **DG7** are isolated and subjected to excitation energy calculations via the hh-tda/b3lyp/def2-svp method. As expected, the shape of the **DG7** is slightly distorted (**Figure S9a)**, leading to a Gaussian-like distribution of the energy gap T_1-T_2 ranging from roughly 0.26 eV to about 0.52 eV (**Figure S9e,f**). The average value of 0.43 eV agrees very well with the T_2-T_1 gap value calculated at the minimized geometry. Careful inspection of the different conformers exhibiting low T_2-T_1 gaps indicates that distortions in **DG7** can make one of the indolocarbazole arms adopt a saddle-like structure as illustrated in **Figure S9a**. In these distorted DG7 conformations, the electronic transitions corresponding to T_2 dominantly involve MOs localized in one of the arms of indolocarbazole as shown in **Figure 6f**, which in turn leads to a decrease in T_2 (from 3.18 eV to 3.06 eV) but an increase in T_1 (from 2.73 eV to 2.79 eV), hence resulting in reduced T_1-T_2 energy splitting as compared to the no-distorted molecules.

This conformational distortion might consequently constitute a possible channel facilitating the internal up-conversion from T_1 to T_2, which could open the way to $T_2 \rightarrow S_2$ rISC or $T_2 \rightarrow T_3 \rightarrow S_1$ IC and rISC, hence to the activation of DF, as observed when **DG7** is doped in Zeonex.

Excitation spectra

Aiming at understanding the absence of the delayed FL in solutions of **DG7**, we have scanned the excitation wavelength from 300-570 nm in different conditions. **Figure S5a, b** corresponds to the PL spectra at different conditions obtained by utilizing excitation wavelengths of 350 nm (3.55 eV) and 530 nm (2.34 eV), respectively. While the general shapes and the intensity trends in different conditions are practically identical in the two figures, the absolute intensities are 3-4 times lower when exciting at higher energy (3.55 eV) than at low energy (2.34 eV). This result is confirmed by the results shown in the **Figures S6**, in which, by scanning the excitation wavelengths from 300-570 nm, we track the intensity of the PL signals at 570 nm and 600 nm, respectively. In **Figure S6a, b**, the presence of two "excitation bands" peaking at the excitation wavelengths of roughly 400nm and 540 nm, separated by a zero-intensity emission around excitation at 450 nm, provides information on the largest- and lowest energy values of the closely-laying excited states S2-S4 (2.76-3.55 eV) and S1 (2.18-2.61 eV), respectively. The theoretical hh-TDA (SCS-CC2) values of 2.81 (2.94) eV and 3.28 (3.42) eV for S1 and S2, respectively, are in reasonable agreement with the above experimental estimations.

Table S1. Vertical excitation energies and their corresponding oscillator strength computed at the SCS-CC2/cc-pVDZ level for **DG7**. The molecular orbitals that describe the low-lying singlet and triplet excited states and their respective weight are also reported.

State	Excitation Energy (eV)	Oscillator Strength	Contribution
S_1	2.94	0.701	HOMO → LUMO (80%)
S_2	3.42	0.001	HOMO-3 → LUMO (37%) HOMO → LUMO+1 (30%)
T_1	2.85		HOMO → LUMO (82%)
T_2	3.16		HOMO-2 → LUMO (33%) HOMO → LUMO+1 (17%)
T_3	3.17		HOMO-1→ LUMO (41%)

			HOMO-2 → LUMO+1 (30%)

Table S2. Adiabatic energy with respect to the ground state for **DG7**. These adiabatic energies are calculated at the SCS-CC2/pVDZ level. The energy gap between the S_1 and T_1 optimized structures is also reported.

	$(S_1)_{min}$	$(T_1)_{min}$	ΔE_{ST}
Adiabatic Energy (eV)	2.83	2.72	0.11

Table S3. Thermal, electrochemical, photoelectrical, hole-transporting and photophysical parameters of **DG7**.

Property	Sample	DG7
PLQY, % [a]		68
η_{PF} [b]		0.62
η_{DF} [b]		0.06
τ_{PF}, ns (%) [b]	DG7(1 wt.%): ZEONEX	6 (91.8)
τ_{DF}, μs (%) [b]		1400 (8.2)
$DPEPOk_{PF}$, s^{-1} [b]		1.04×10^8
k_{ISC}, s^{-1} [b]		8.5×10^6
k_{DF}, s^{-1} [b]		40
k_{RISC}, s^{-1} [b]		43

[a] Photoluminescence quantum yield determined using an integrating sphere, [b] deoxygenated toluene solution of compound, [b] obtained by the formula $\eta_{PF} = \eta_{PLQY} * PF(\%)/100(\%)$, $\eta_{DF} = PLQY * DF(\%)/100(\%)$; from PL decay fitting by

$$k_{PF} = \frac{\eta_{PF}}{\tau_{PF}}; \quad k_{ISC} = \frac{\eta_{DF}}{\eta_{PF} + \eta_{DF}}k_{PF}; \quad k_{DF} = \frac{\eta_{DF}}{\tau_{DF}}; \quad k_{RISC} = \frac{\eta_{DF}}{\eta_{PF}} \cdot \frac{k_{PF}.k_{DF}}{k_{ISC}}.$$

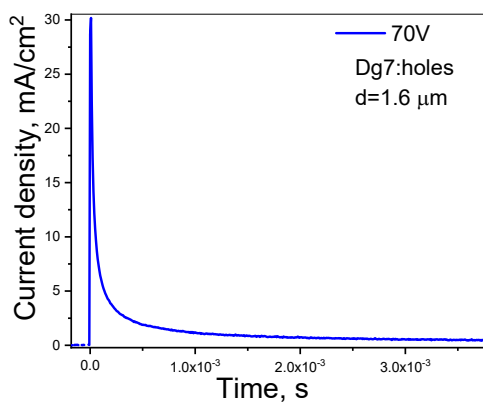I=A+B1exp(-t/τ_{PR})+B2exp(-t/τ_{DF}) (**Figure 6a, b**); [f] Singlet (E_S) and triplet (E_T) energies estimated from onsets of the fluorescence and phosphorescence spectra at 77 K recorded in THF solutions.
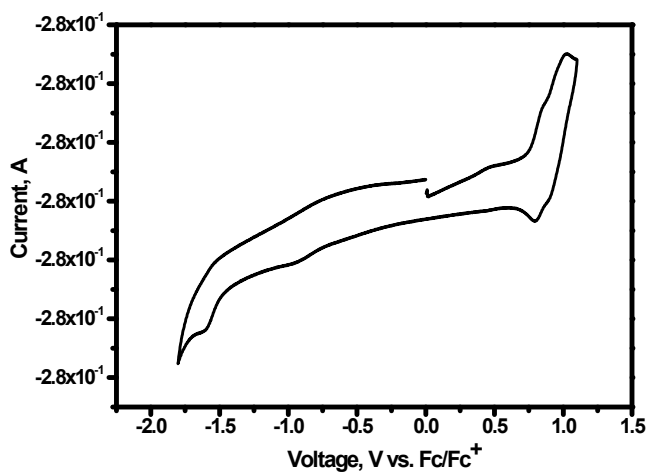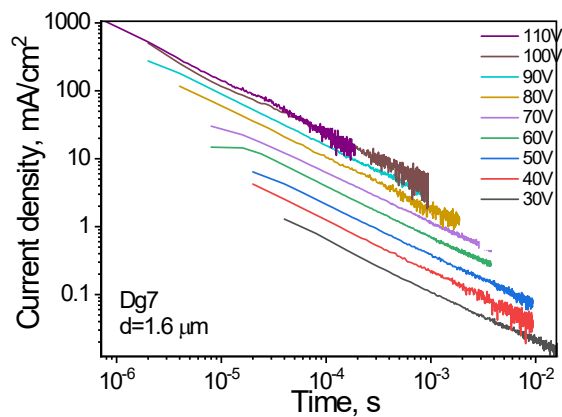
(a)
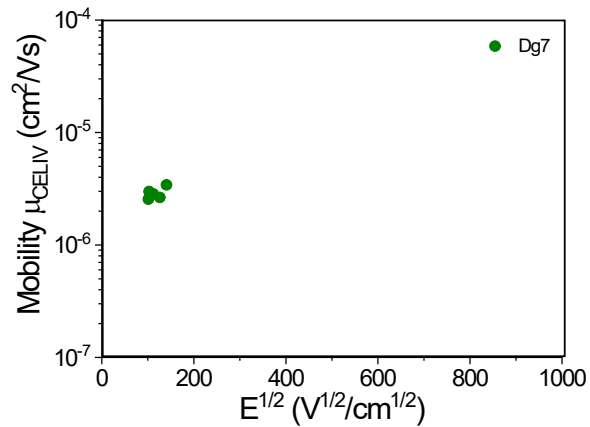
(b)

(c)

(d)

Figure S1. Cyclic voltammperogram (a), hole mobility (b) as the function of electric fields, TOF signals in linear (c) and log-log (d) scales of the vacuum-deposited film of **DG7**.
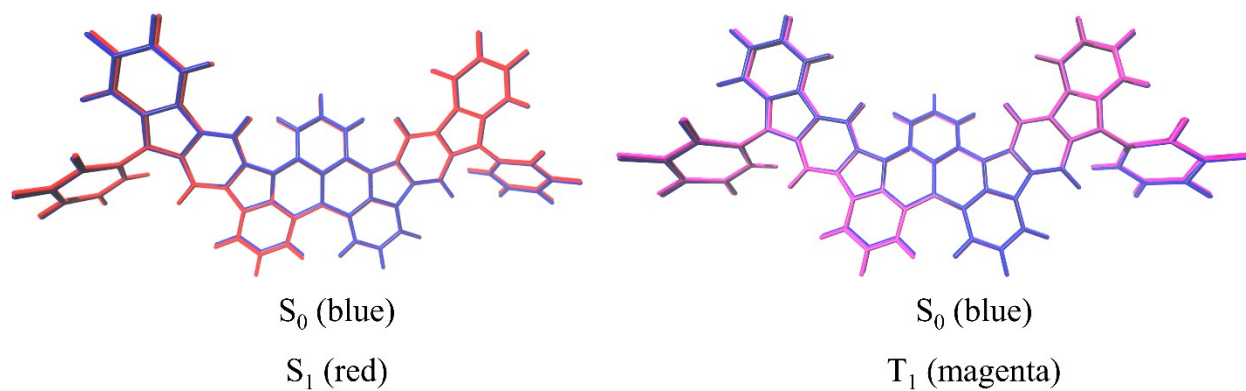
S₀ (blue)

S₁ (red)

S₀ (blue)

T₁ (magenta)

Figure S2. Superimposition of the optimized structures of **DG7**.

(a)

$S_0 \rightarrow S_1$

(b)

Frequency = 25 cm^{-1}

$S_j = 2.3$
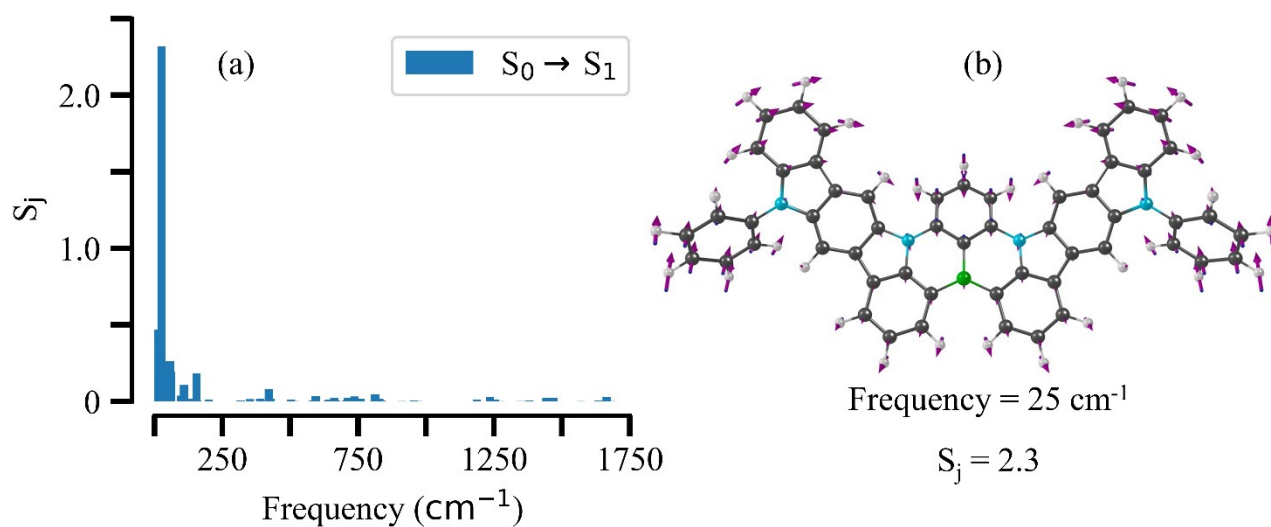
Figure S3. (a) Huang-Rhys factor magnitude as a function of the vibrational normal model of **DG7** and (b) normal model that has the highest Huang-Rhys factors value.
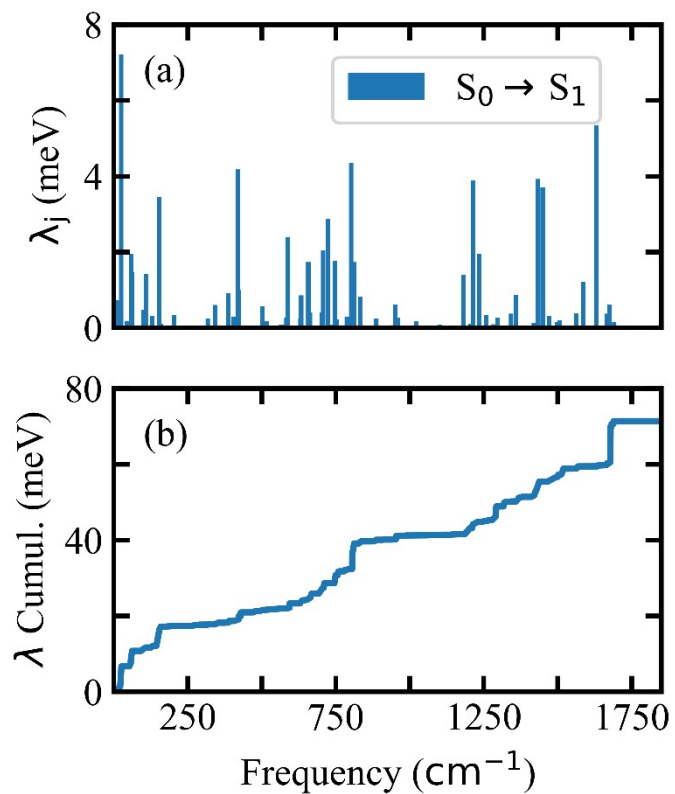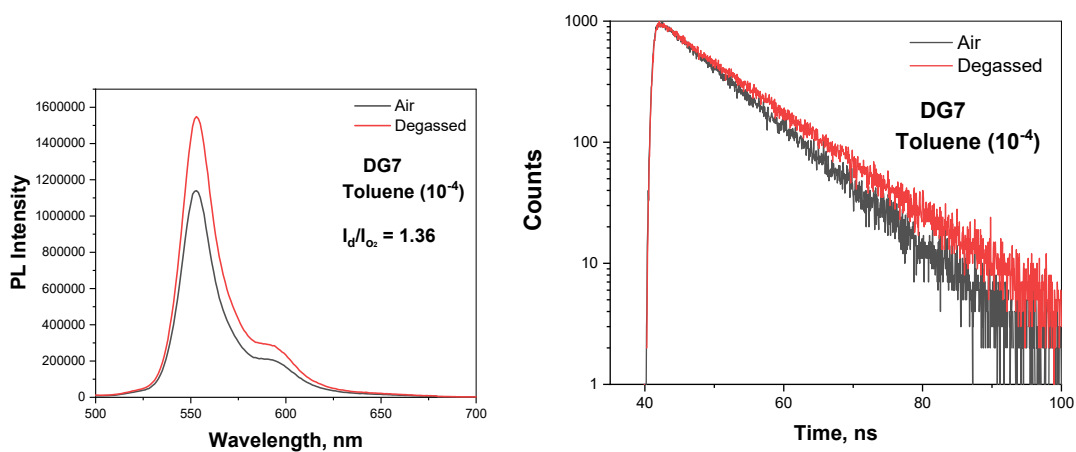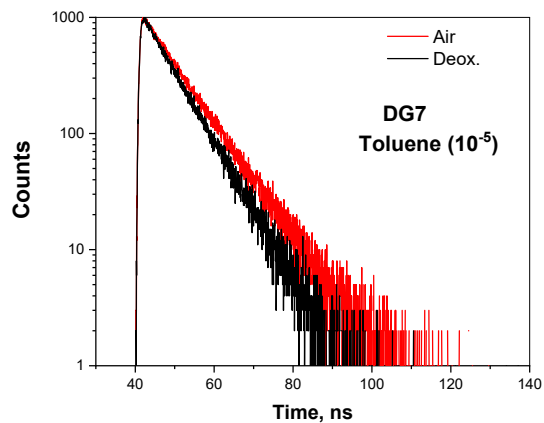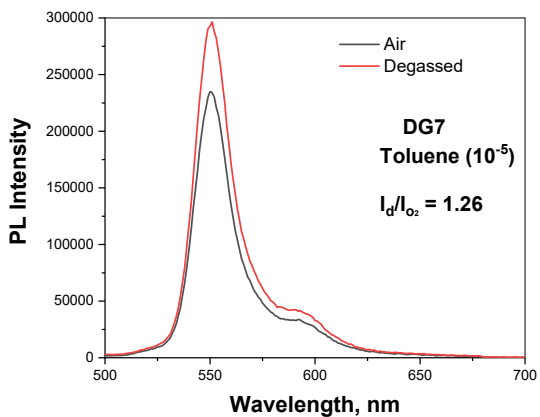
Figure S4. (a) Reorganization energy per mode and (b) cumulative reorganization energy in meV with respect to the frequency in cm^{-1}.

DG7
Toluene (10^{-5})
After sonification
$I_d/I_{O_2} = 1.37$

DG7
After sonification
Toluene (10^{-5})

DG7
Toluene (10^{-5})
$I_{sd}/I_{O_2} = 2.1$

DG7
Toluene (10^{-5})

DG7
Toluene (10^{-6})
$I_d/I_{O_2} = 1.33$

DG7
Toluene (10^{-6})
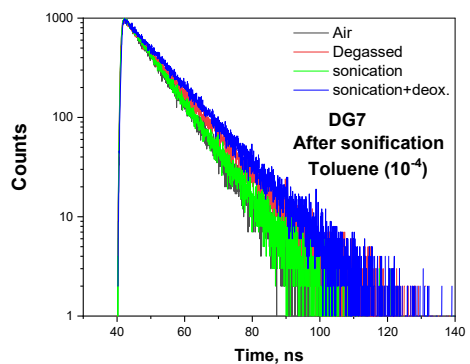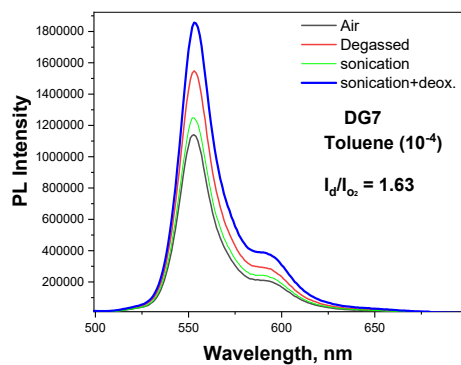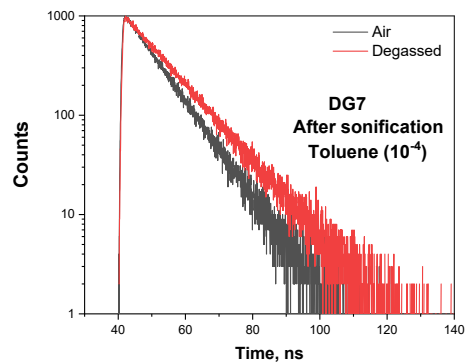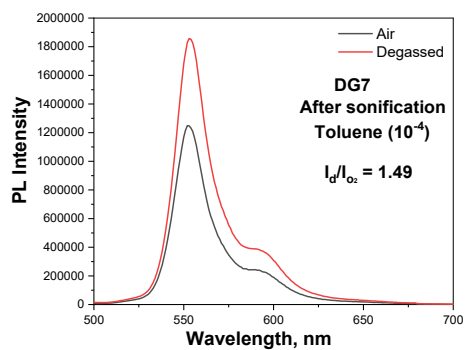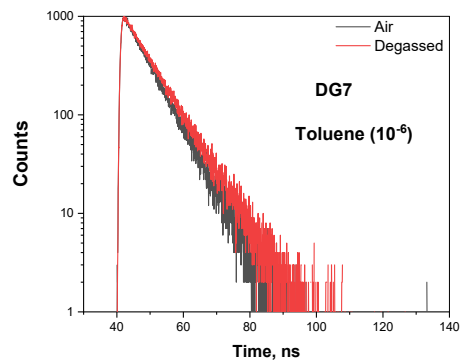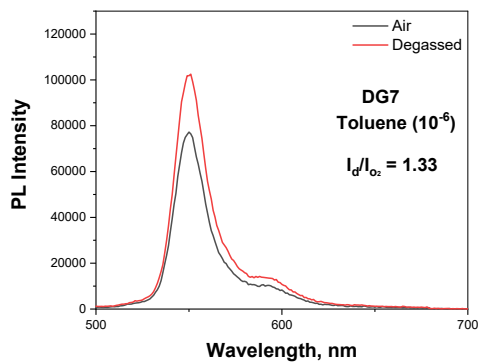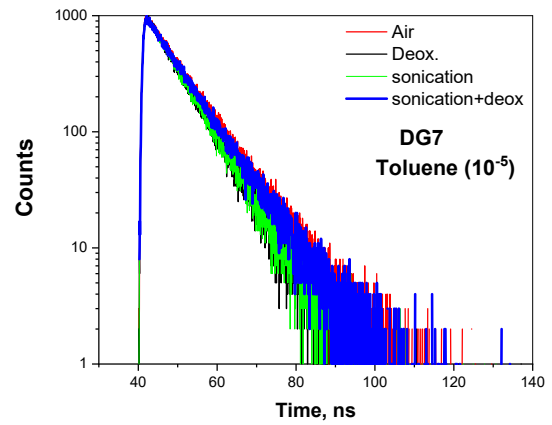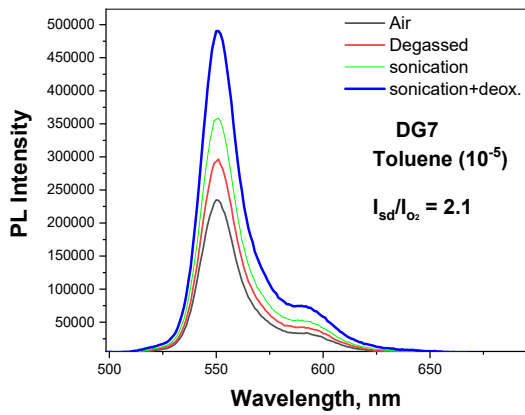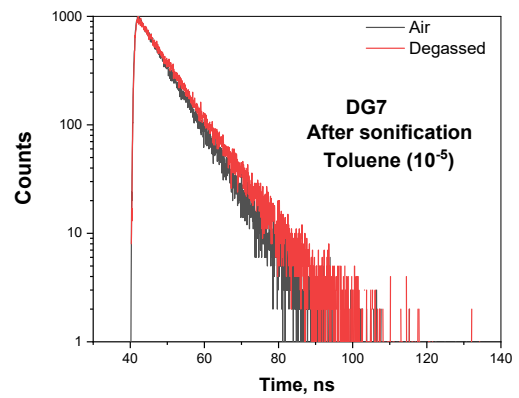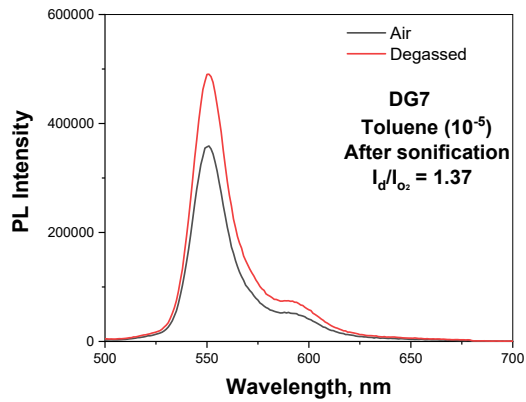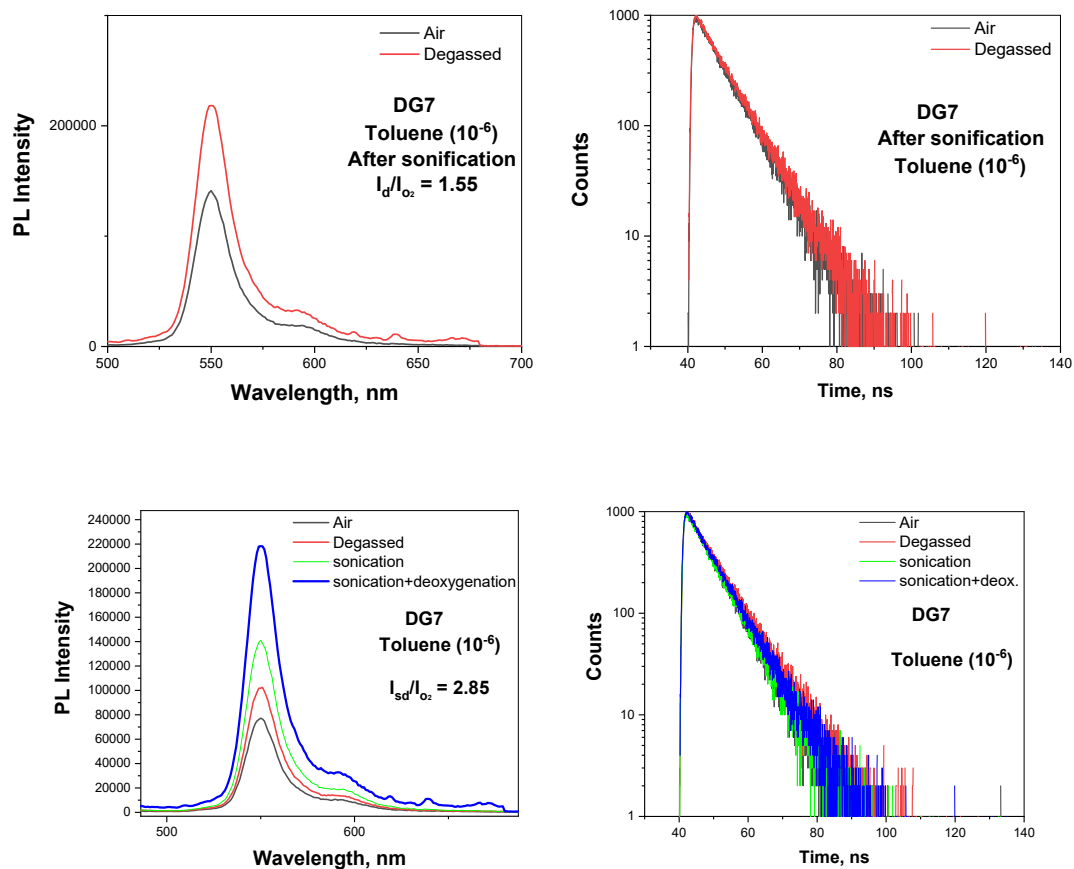
Figure S5. Air-equilibrated (Air) and deoxygenated (degassed) PL spectra (left) and PL decay curves (right) before and after an ultrasonic bath for toluene solutions of **DG7** of different concentrations.

(a) (b)
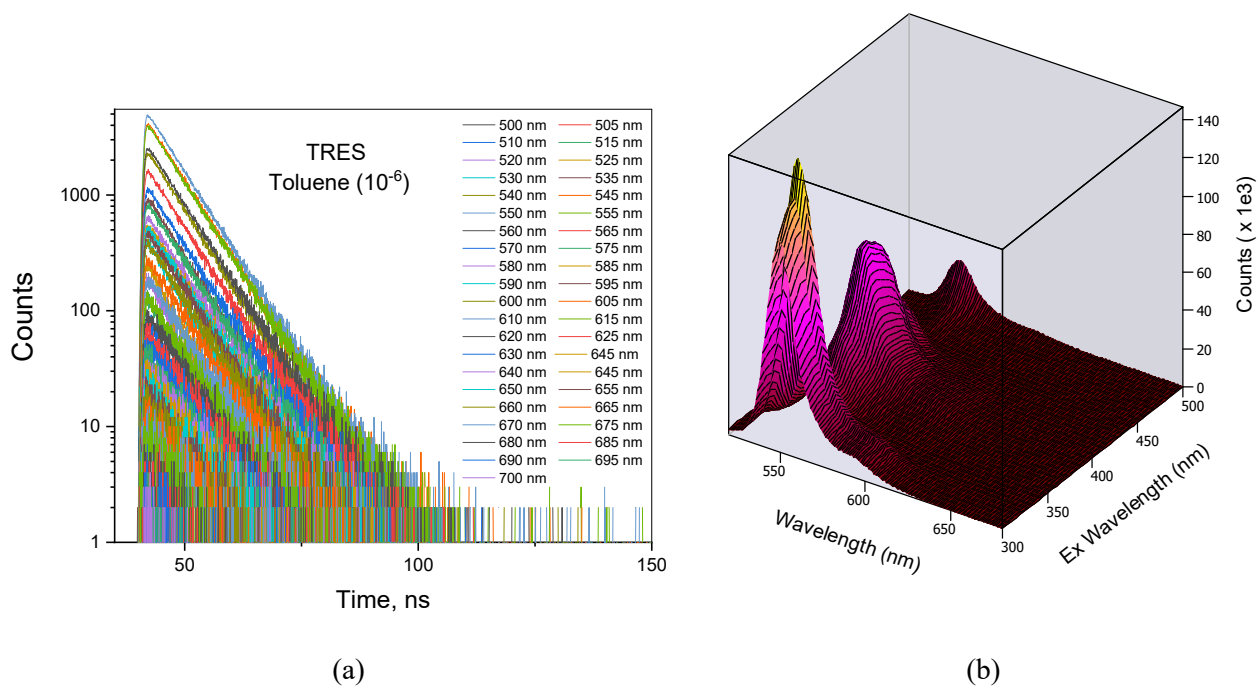
Figure S6. PL decay curves of time-resolved emission spectra (TRES) of DG7 in toluene (10^{-6}) from 500-700 nm (a). PL spectra mapping of DG7 in toluene (10^{-6}) at excitation of 300-500 nm (b).

(a) (b)
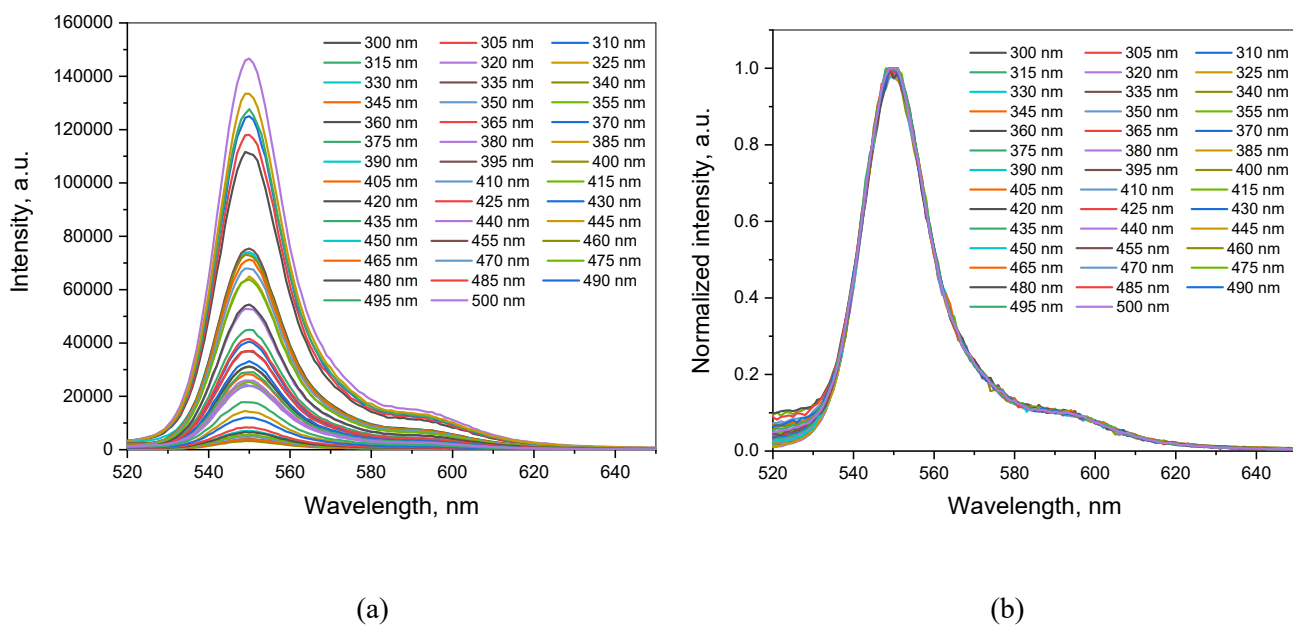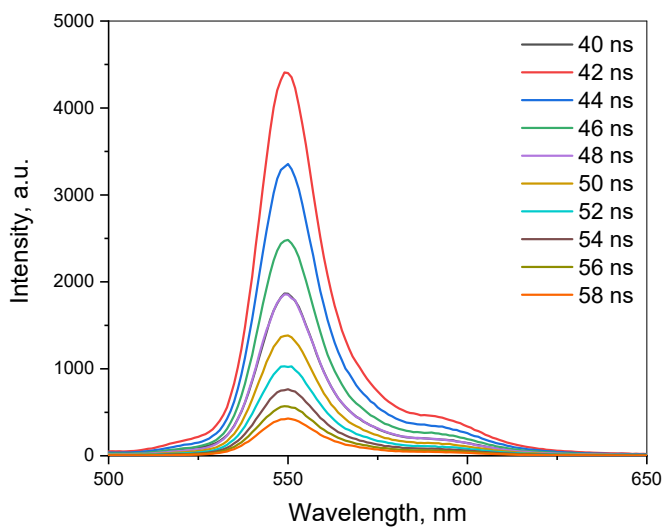
(c)
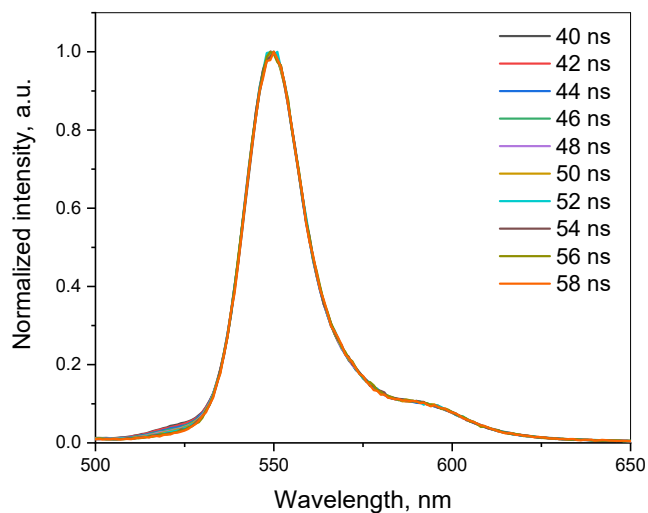
(d)

Figure S7. PL spectra (a) and normalized PL spectra (b) of excitation scan of **DG7** in toluene (10^{-6}) from 300-500 nm (a-c). Selected emission spectra recorded at the different delays (40-58 ns) after excitation obtained from time-resolved emission spectra (TRES) of **DG7** in toluene (10^{-6}) from 500-650 nm.
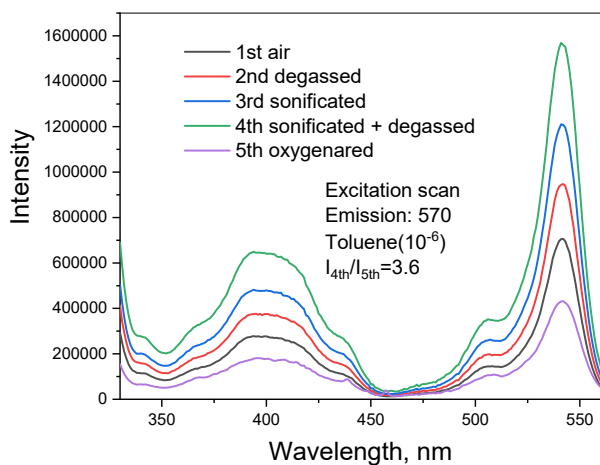
(a)
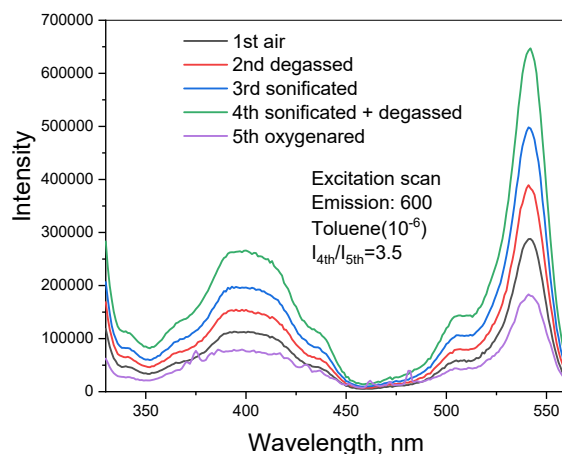
(b)

Figure S8. (a,b) Excitation scans of **DG7** in toluene (10^{-6}) from 330 to 560 nm at the emission of (a) 570 nm and (b) 600 nm, for 5 different conditions of solution.

(a) Conformational Distortion

(b) LUMO

(c) HOMO

(d) HOMO-1

(e)

(f)
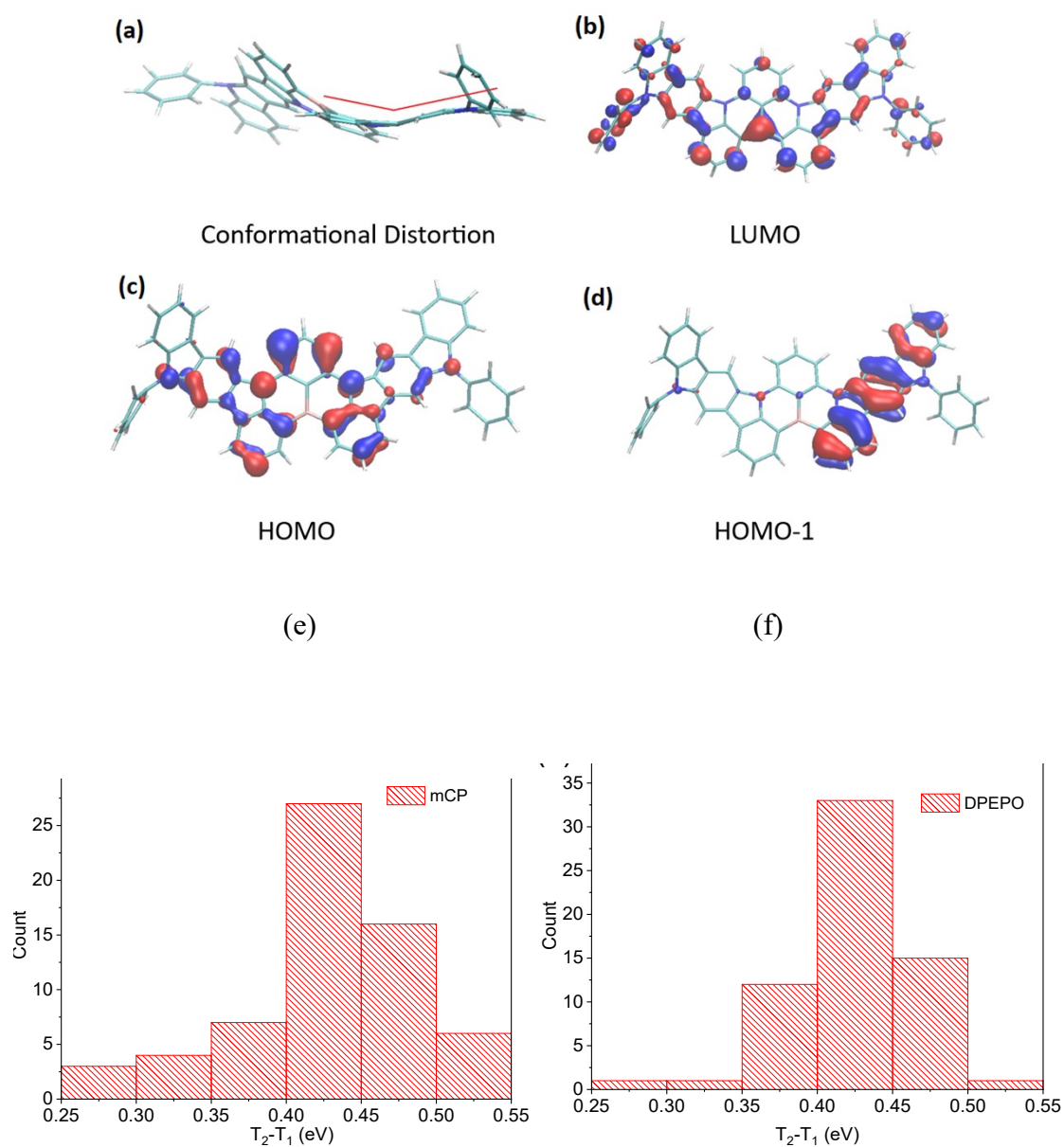
Figure S9: (a) The conformational distortion of one of the indocarbazole arms, as extracted from the MD with **DG7** doped in DPEPO, denoted by the red line highlighting the saddled structure. The hh-tda/b3lyp/def2-svp results for (b) LUMO, (c) HOMO, and (d) HOMO-1. The $S_0 \to T_1$ is dominated by HOMO $\to$ LUMO transition while $S_o \to T_2$ is dominated by HOMO-1 $\to$ LUMO transition. Similar behavior is seen in **DG7** doped in mCP.

Frequency distribution of T_2-T_1 energy gap of **DG7,** calculated using hh-tda/b3lyp/de2-svp on the molecular configurations extracted from molecular dynamics simulations on the mixtures of DG7 (8%) with (e) mCP and (f) DPEPO
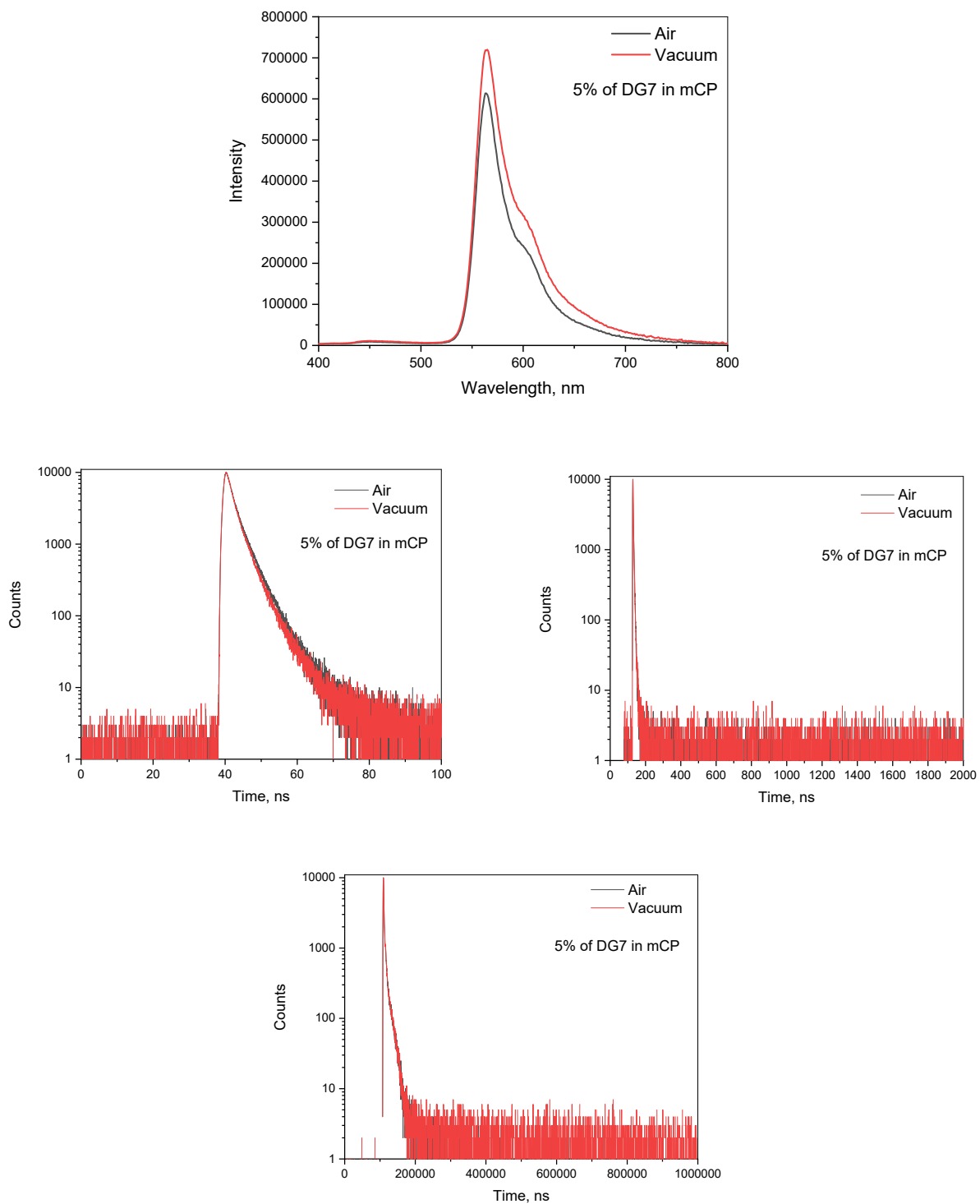
Figure S10. PL spectra and PL decay curves of DG7 film dispersed in mCP host (5%) in the air and vacuum
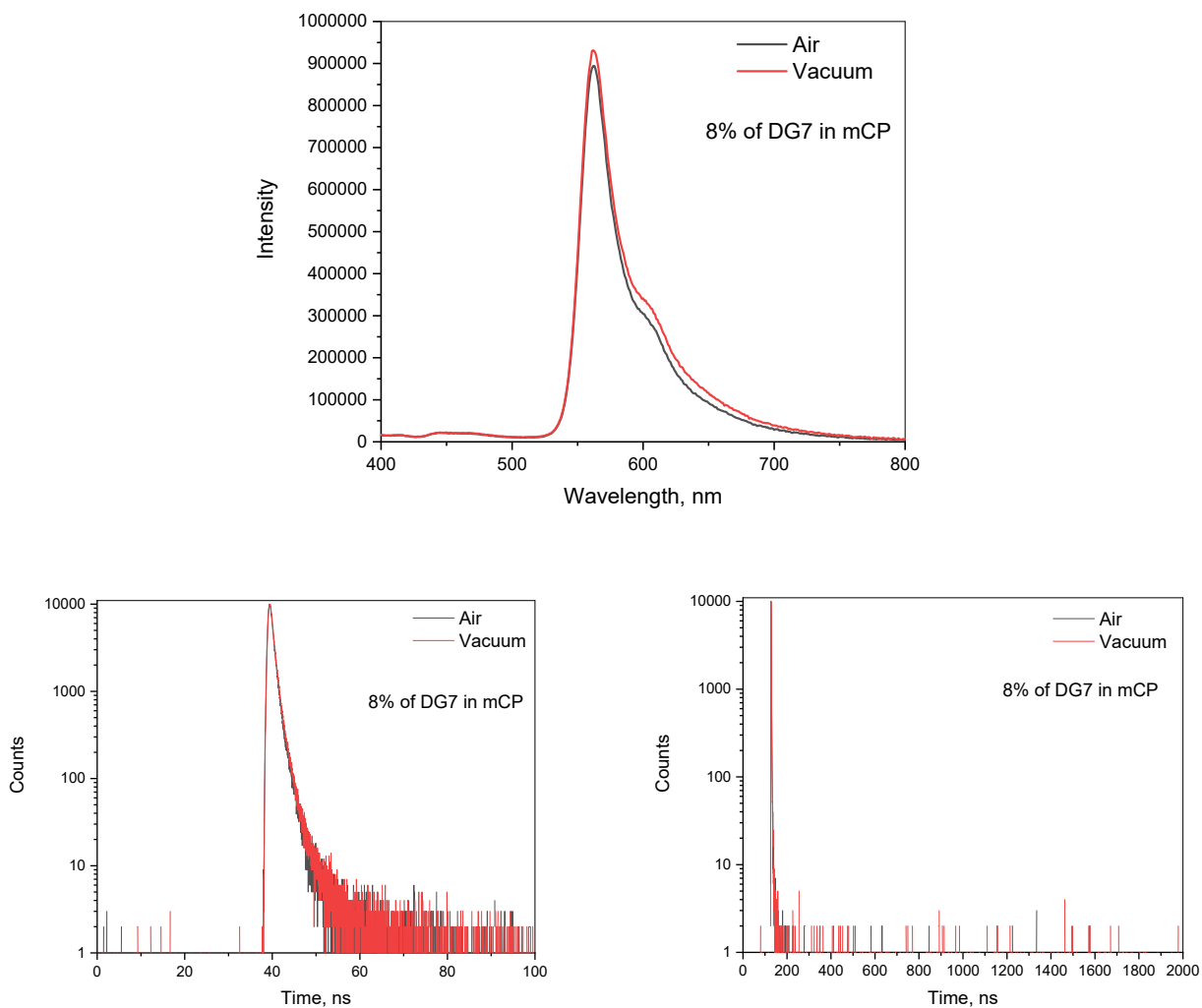
Figure S11. PL spectra and PL decay curves of DG7 film dispersed in mCP host (8%) in the air and vacuum
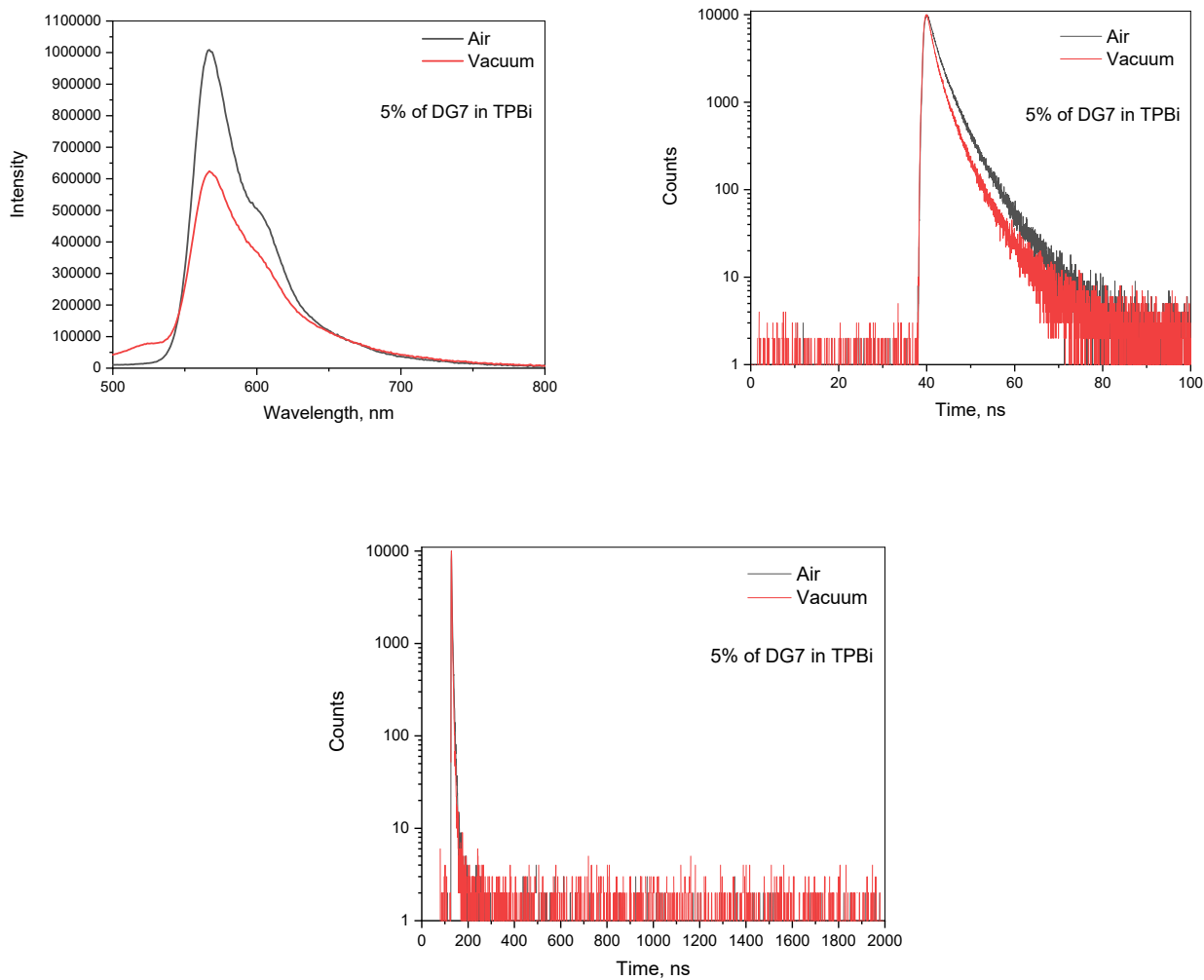
Figure S12. PL spectra and PL decay curves of DG7 film dispersed in TPBi host (5%) in the air and vacuum
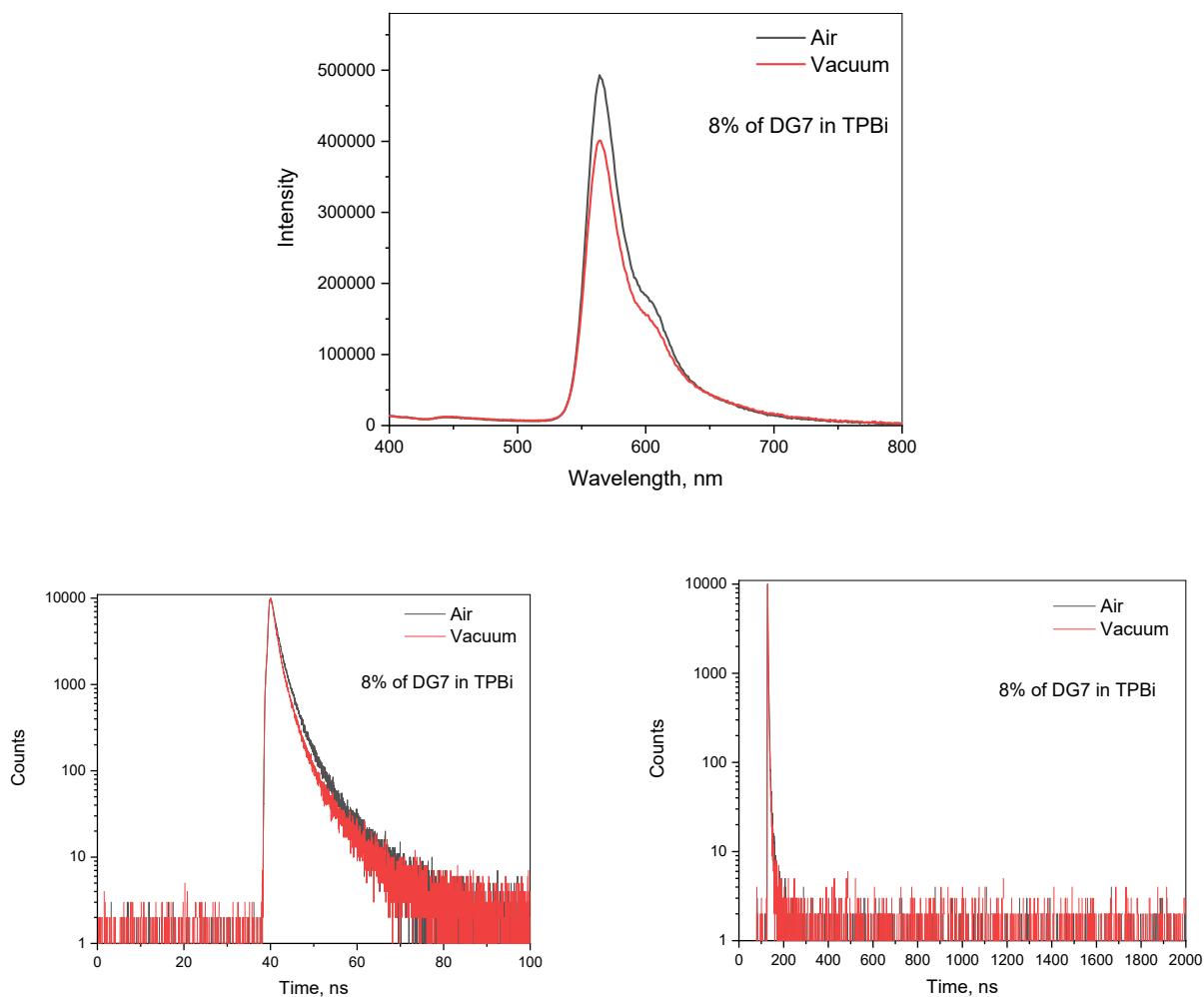
Figure S13. PL spectra and PL decay curves of DG7 film dispersed in TPBi host (8%) in the air and vacuum
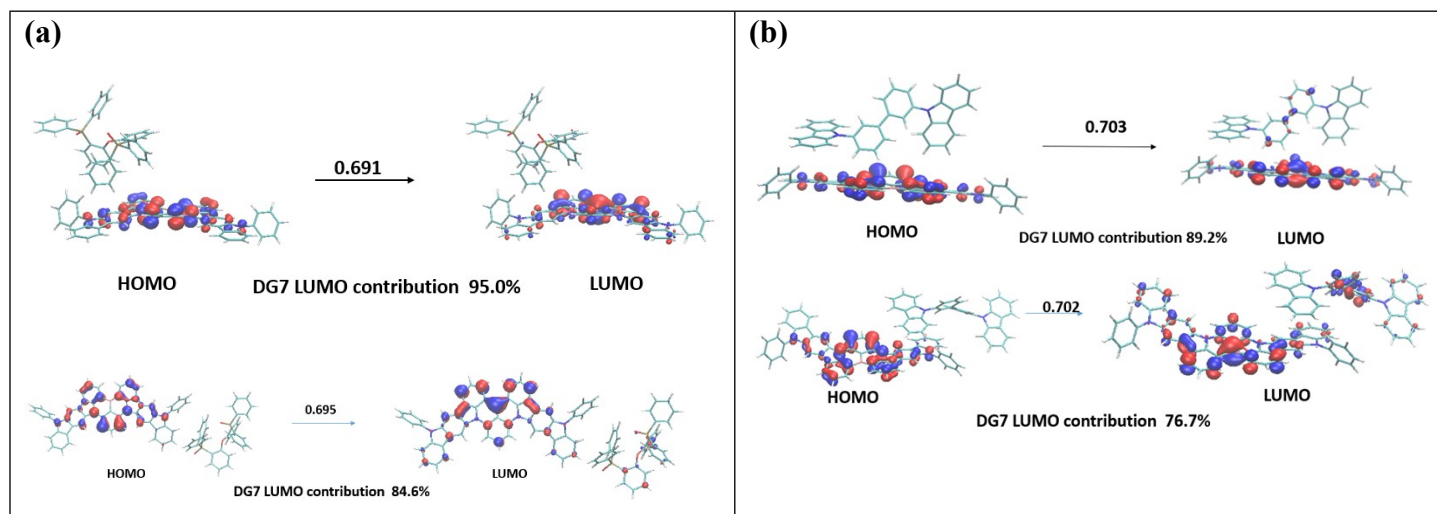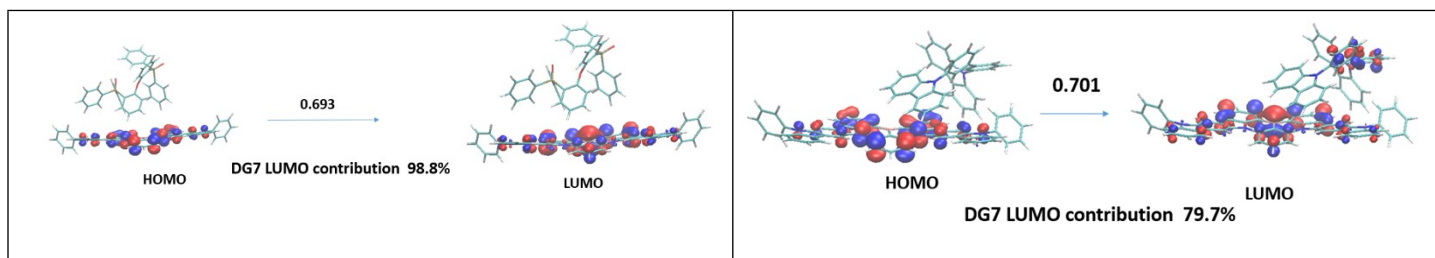
Figure S14: More examples of (a) **DG7**-DPEPO and (b) **DG7**-mCBP complexes extracted from molecular dynamic simulations.
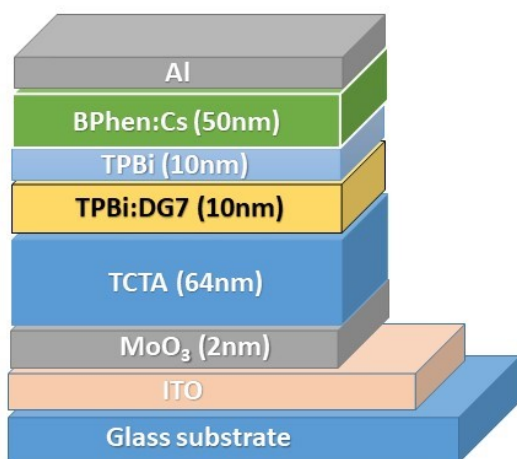
(a)
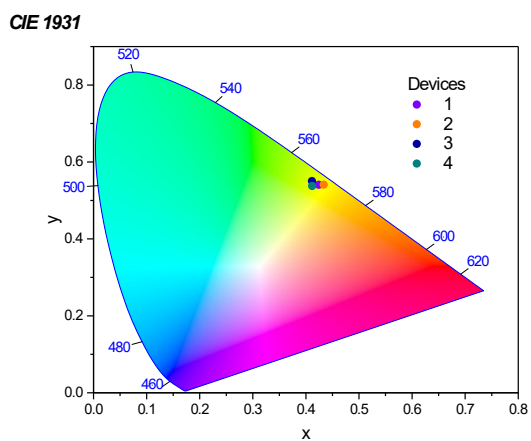
(b)
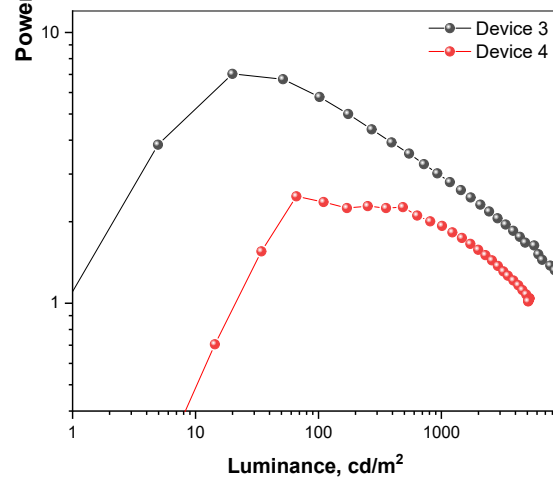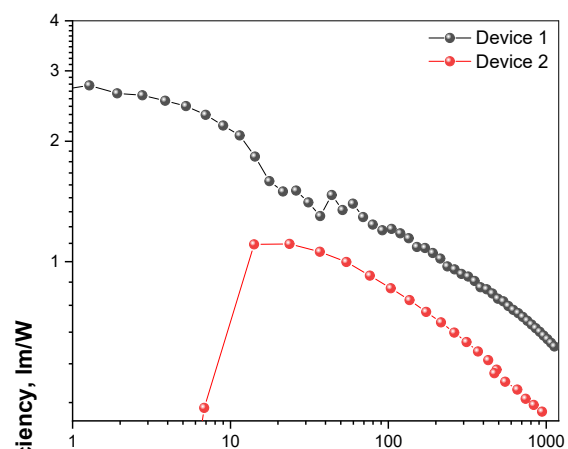
(c)

Figure S15. Device structure (a), CIE colour coordinates (b) and power efficiency versus luminance (c) of **DG7**-based OLEDs.
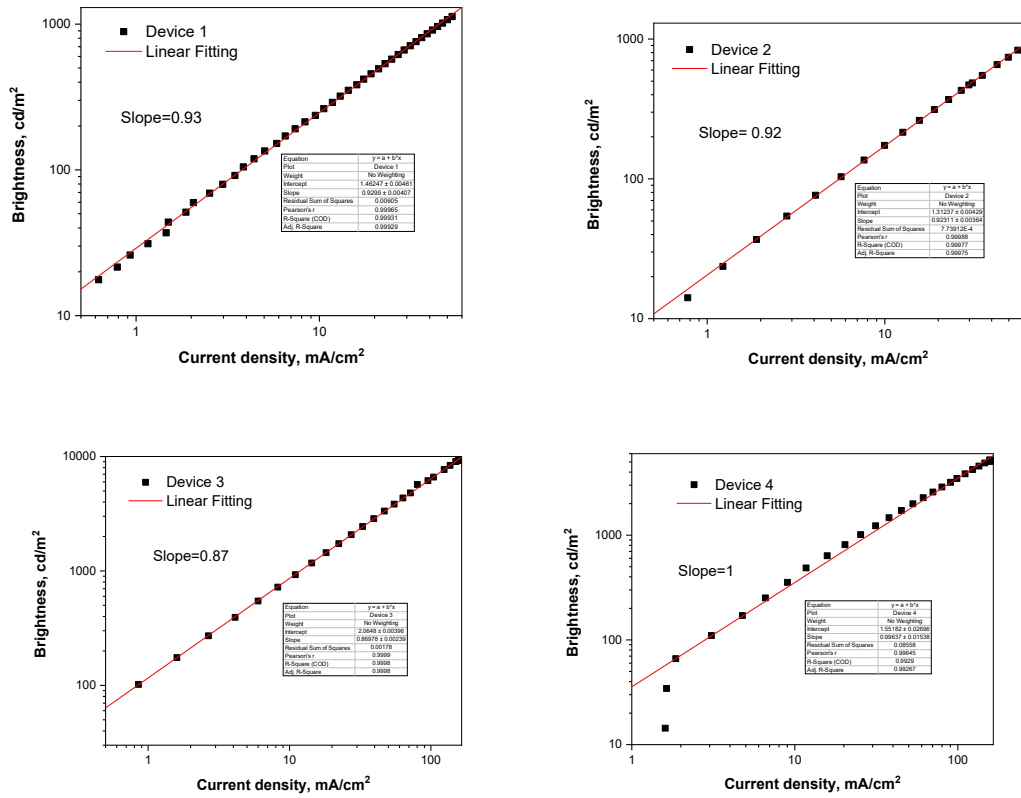
Figure S16. Linear fits to current density versus brightness plots for devices 1-4

(a)
(b)
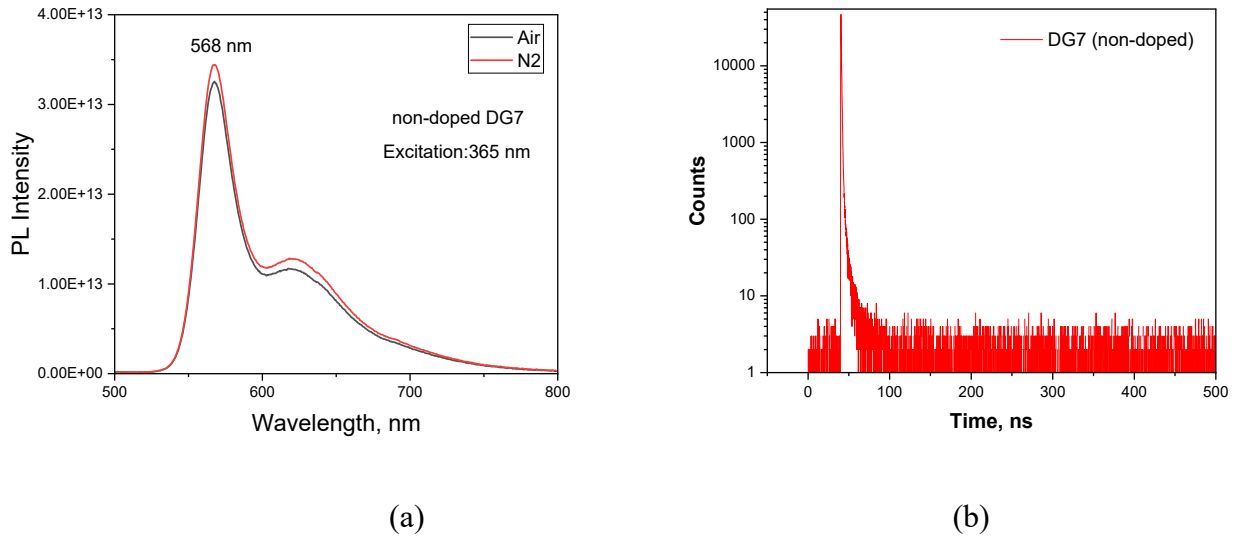
Figure S17. PL spectra and PL decay curves of **DG7** neat film in air equilibrated and N_2 atmosphere

Optimized Ground State using XYZ Coordinate of Molecular Structure Used to carry out hh-TDA

DG7

90

-2.3188915720516411e+03 frame 0   xyz file generated by TeraChem

C	-2.6542738555	-0.6511842223	0.2309656648
C	-2.6702190024	0.3219924586	1.2304391119
C	-2.2758196809	1.6423617708	0.9109542850
C	-1.9209445076	2.0606576316	-0.3820029445
C	-1.9051040307	1.0372860961	-1.3593367714
C	-2.2538847311	-0.2849740434	-1.0632541589
C	-3.0427921327	0.3266377541	2.6305541999
C	-2.8514045640	1.6633687704	3.1130521287
N	-2.3242553737	2.4486157706	2.0477739187
C	-3.5636353730	-0.6857242497	3.4391240644
C	-3.9019002591	-0.3428792395	4.7487542597
C	-3.7642299477	0.9918116560	5.2285357179
C	-3.2458843107	2.0071213777	4.4088271280
B	-1.6267758961	3.5681568286	-0.5347109240
C	-1.4534941196	4.3896435558	-1.8297522679
C	-1.4892011573	4.3603370867	0.7838248966
C	-1.8253273607	3.7619324919	2.0438827350
C	-1.6366525929	4.4714336556	3.2416417893
C	-1.2345851537	5.8035702101	3.1917756392
C	-0.9561386203	6.4438237288	1.9871733362
C	-1.0220961558	5.7170399603	0.7866022020
C	-0.9538703855	5.6910825809	-1.6578946813
N	-0.6586227247	6.3008201387	-0.4383687841
C	-0.0632907865	7.5640272596	-0.7197135145
C	-0.0823162121	7.7612581060	-2.1398925969
C	-0.6522412295	6.5659684966	-2.7277012269
C	0.5489396609	8.5049725982	0.1124036527
C	1.0705424062	9.6657201662	-0.4808897222

28

C	0.9952850746	9.8706863302	-1.8891547066
C	0.4392656374	8.9112468227	-2.7361499175
C	-0.9122644737	6.1539054216	-4.0349304523
C	-1.4587818737	4.8787574431	-4.2461440201
C	-1.7140127246	4.0205567442	-3.1709040005
C	1.7598412629	10.8172987909	0.0683515286
C	2.0720517072	11.6709530417	-1.0259798734
N	1.6044269901	11.0897015620	-2.2071337125
C	2.1196104780	11.2017009846	1.3687714606
C	2.7734666798	12.4184522553	1.5628630357
C	3.0628750483	13.2580916709	0.4696712966
C	2.7163066423	12.9003169940	-0.8344519532
C	1.7626440560	11.6185373855	-3.5162272418
C	0.6390211875	11.8605665446	-4.3224636554
C	0.8025363929	12.3701422964	-5.6135897763
C	2.0810888991	12.6593412498	-6.1022448098
C	3.2004345069	12.4263284244	-5.2958996352
C	3.0462326161	11.8990761339	-4.0112195211
N	-4.4623032859	-1.1357680743	5.7563776902
C	-4.6877282664	-0.3320406505	6.8766777136
C	-4.2663902059	0.9960541849	6.5890077900
C	-5.2021206046	-0.6809625863	8.1321146589
C	-5.3064364511	0.3238733171	9.0956955181
C	-4.9049157396	1.6462478663	8.8237112327
C	-4.3816608088	1.9862245387	7.5762309866
C	-4.7918873833	-2.5126131622	5.6370359302
C	-3.7973544482	-3.4531622118	5.3251631015
C	-4.1293081703	-4.8047034271	5.1959238738
C	-5.4471431167	-5.2302761091	5.3938858610
C	-6.4371673750	-4.2945741871	5.7121798540
C	-6.1165288349	-2.9392132152	5.8245795360
H	-2.9453578544	-1.6822767795	0.4500038693

H	-1.5981169685	1.2805288027	-2.3785296794
H	-2.2230928340	-1.0411968317	-1.8519214610
H	-3.7181767835	-1.6931370388	3.0489361779
H	-3.2107756937	3.0247174303	4.7882607281
H	-1.7762801364	3.9968843401	4.2064655118
H	-1.1346463098	6.3633235115	4.1258143768
H	-0.7139415227	7.5005558498	1.9940372688
H	0.6753349332	8.3574432937	1.1815552673
H	0.4285534742	9.0357259770	-3.8203164678
H	-0.6980454455	6.8120290799	-4.8815908000
H	-1.6807785206	4.5495954928	-5.2645752095
H	-2.1432801256	3.0382287266	-3.3781429638
H	1.8867813777	10.5569930915	2.2207743940
H	3.0603856169	12.7273427329	2.5711428500
H	3.5671096780	14.2127527601	0.6429119662
H	2.9361010973	13.5601477210	-1.6759341420
H	-0.3588280985	11.6559916446	-3.9273515232
H	-0.0774476304	12.5541970122	-6.2358675882
H	2.2051832551	13.0655153905	-7.1093688213
H	4.2035488243	12.6437636182	-5.6726612002
H	3.9181117510	11.6923747264	-3.3862823552
H	-5.5082807116	-1.7053960125	8.3529291454
H	-5.7059583795	0.0747460316	10.0825633890
H	-5.0005811779	2.4095225752	9.5999826592
H	-4.0615398581	3.0115867648	7.3713700768
H	-2.7653116983	-3.1194335226	5.1940681319
H	-3.3488341448	-5.5304355984	4.9517917214
H	-5.7021235226	-6.2889820978	5.3000642142
H	-7.4708636000	-4.6176662405	5.8622178522
H	-6.8912547016	-2.2021656402	6.0484384044

DABNA-1

54

-1.2893990830938296e+03 frame 53   xyz file generated by TeraChem

```
C   -3.8323530719    1.7582569958    0.3391969268
C   -3.9722112084    3.1142423431    0.6071920255
C   -2.8413596618    3.9317898049    0.7535030723
C   -1.5816613036    3.3709498856    0.5731522338
C   -1.3825897379    2.0041489204    0.2538283475
C   -2.5466577814    1.1780005128    0.1946413777
B   -0.0003507374    1.3411394013    0.0005150064
C    0.0005029470   -0.1809802901    0.0006245833
C   -1.2253863608   -0.9089304637    0.0002467483
N   -2.4411532666   -0.2112154809    0.0089998373
C    1.2271648240   -0.9075460358    0.0009191039
C    1.2215268308   -2.3176244605    0.0161944758
C    0.0020602458   -2.9911015714    0.0003701085
C   -1.2182821219   -2.3189558076   -0.0152981110
C    1.3813640974    2.0053484902   -0.2531476510
C    2.5464695813    1.1808558859   -0.1938355904
N    2.4423739538   -0.2085111317   -0.0077632380
C    1.5791520551    3.3724666203   -0.5733618329
C    2.8379206269    3.9344148131   -0.7542619845
C    3.9700227014    3.1181895709   -0.6075734939
C    3.8314988395    1.7625220473   -0.3387604140
C   -5.9651849354   -2.5392025091   -0.3120427150
C   -5.3463725593   -2.0417430914   -1.4628134098
C   -4.1889823842   -1.2652844711   -1.3581746531
C   -3.6487835953   -0.9861779220   -0.0973951645
C   -4.2677253656   -1.4828747916    1.0565997734
C   -5.4246455422   -2.2577205326    0.9469070191
C    4.2688896493   -1.4792906023   -1.0565816526
C    3.6505613472   -0.9830912844    0.0978629248
C    4.1906507709   -1.2638319885    1.3583490118
```

C	5.3468942882	-2.0421269629	1.4622029831
C	5.9647650609	-2.5397360557	0.3110013887
C	5.4247097981	-2.2560503835	-0.9476091828
H	-4.7257289095	1.1400054112	0.2580274318
H	-4.9762766367	3.5335080687	0.7223754432
H	-2.9490041807	4.9911673459	1.0030806709
H	-0.7044893503	4.0081876424	0.7032662265
H	2.1490222523	-2.8862194349	0.0256725061
H	0.0026704462	-4.0852831647	0.0002181180
H	-2.1452828948	-2.8884208471	-0.0249243796
H	0.7012510947	4.0086576124	-0.7037596867
H	2.9443799368	4.9936926297	-1.0046033399
H	4.9735425168	3.5385738452	-0.7231812689
H	4.7254457488	1.1451332373	-0.2572789596
H	-6.8681112569	-3.1470915568	-0.3959659547
H	-5.7631337712	-2.2602830620	-2.4481473190
H	-3.6941389150	-0.8764973552	-2.2520260853
H	-3.8335220803	-1.2624700358	2.0353470881
H	-5.9023874361	-2.6457978036	1.8487028622
H	3.8349568729	-1.2577167499	-2.0350925677
H	3.6964348507	-0.8754216198	2.2526632111
H	5.7632826188	-2.2623093318	2.4473499743
H	6.8665664632	-3.1495527591	0.3943884628
H	5.9016847656	-2.6442021948	-1.8498300114

Model 1

94

-2.4485013895484726e+03 frame 120   xyz file generated by TeraChem

C	2.9076173314	1.1400263833	0.4165656895
C	4.0470130436	0.4580234097	0.8850847657
C	4.0128035679	-0.8829563845	1.2616274300
C	2.8290592436	-1.5948200257	1.0885725392

```
C    1.6455209019   -0.9965981863    0.6096073285
C    1.6734349756    0.4144522368    0.3794489957
B    0.3437853712   -1.7799863706    0.3352003941
C   -0.8708212757   -0.9291508169    0.0075179316
C   -0.7219326995    0.4563455393   -0.2422082454
N    0.4738205369    1.1151454402    0.1374703339
C   -2.1123188692   -1.5542517632   -0.2595987716
C   -3.1350213044   -0.8483654612   -0.9070808523
C   -2.9182554224    0.4860699261   -1.2541636029
C   -1.7395267839    1.1514256300   -0.9195689761
C    0.1317633686   -3.3002382673    0.1239744041
C   -1.1989799980   -3.8123991618    0.0185891927
N   -2.2871858082   -2.9177480925    0.0919448289
C    1.1898357903   -4.2189347355   -0.0296485298
C    0.9762781928   -5.5840270288   -0.2029651367
C   -0.3325533267   -6.0605759419   -0.2524272547
C   -1.4485546499   -5.2065583621   -0.1745357723
B   -2.9109560545   -5.7134373686   -0.2284915324
C   -3.9272835781   -4.7126674198    0.2931716700
C   -3.5674969877   -3.3599854640    0.5084191126
C   -3.4763420257   -7.0951594223   -0.6318407937
C   -4.8257675739   -7.3801739916   -0.2670272142
N   -5.5960323943   -6.4422293894    0.3929075666
C   -5.2336961482   -5.1389131656    0.6494132037
C   -6.1413218745   -4.2547870040    1.2609404133
C   -5.7293503533   -2.9503888107    1.5198285849
C   -4.4590881443   -2.4893889620    1.1538748380
C   -2.7920391607   -8.0975701182   -1.3625130977
C   -3.3727986824   -9.3178354556   -1.6845742863
C   -4.6913858223   -9.5851154770   -1.2719846548
C   -5.4135952985   -8.6285242128   -0.5745052597
C    0.4211670045    2.5162953579    0.3948251393
```

C	1.5620393925	3.3055295614	0.1201665441
B	2.9193625613	2.6346362802	0.0151553716
C	-0.7124777235	3.1005803052	0.9743160761
C	-0.7125625659	4.4751505305	1.2229597541
C	0.3574684820	5.2896660458	0.8557856951
C	1.4911129909	4.7116002770	0.2583174691
N	2.5923501087	5.5152680279	-0.1387953430
C	3.9068880845	4.9936150390	-0.1889179655
C	4.1156239322	3.5793345013	-0.2160383735
C	5.0189797598	5.8923523401	-0.2110550527
C	6.3011878978	5.3500713571	-0.4137596255
C	6.5141405106	3.9819935952	-0.5757657800
C	5.4281441636	3.1201520518	-0.4521888290
C	2.3352952073	6.8445958391	-0.5808138691
C	3.3518699093	7.8198970872	-0.4428160711
B	4.7679784999	7.4115231340	-0.0882864038
C	1.1165639877	7.1946294539	-1.1818333135
C	0.8800064034	8.5277139067	-1.5417132367
C	1.8227900321	9.5285825855	-1.3258696752
C	3.0708885541	9.1684762828	-0.7856449768
N	4.0532612696	10.1159967725	-0.6009842302
C	5.3100304884	9.8875231098	-0.0731433938
C	5.7500655752	8.5621662210	0.2161311407
C	6.1498482092	10.9983287777	0.1679581010
C	7.4103056837	10.8105493828	0.7159541007
C	7.8601307762	9.5173823291	1.0418421975
C	7.0374238680	8.4264709326	0.7901648471
H	4.9818979501	1.0089570362	0.9920635119
H	4.9013731428	-1.3705629552	1.6695986461
H	2.8050246360	-2.6476916136	1.3715477233
H	-4.0728390718	-1.3366457698	-1.1692254666
H	-3.6893821498	1.0220866096	-1.8136082148

H	-1.6105743855	2.1931938834	-1.2067606284
H	2.2148797193	-3.8482851777	-0.0187189883
H	1.8216593776	-6.2699312803	-0.2979588359
H	-0.4987443639	-7.1338557931	-0.3568081078
H	-6.5355508036	-6.7214193080	0.6536205544
H	-7.1428297438	-4.5935726198	1.5377881144
H	-6.4137559635	-2.2633308226	2.0249202847
H	-4.1751385573	-1.4626533126	1.3790725620
H	-1.7762665152	-7.8947143034	-1.7063568151
H	-2.8147665819	-10.0627038210	-2.2571706429
H	-5.1590128807	-10.5437962400	-1.5130266167
H	-6.4461655099	-8.8259066202	-0.2716822533
H	-1.5713056466	2.4955593892	1.2612291133
H	-1.5718844624	4.9239769733	1.7278682451
H	0.3164617919	6.3580479884	1.0597871447
H	7.1511188597	6.0322421992	-0.4779954985
H	7.5142458895	3.5926190746	-0.7811054285
H	5.5924180948	2.0483955508	-0.5725673826
H	0.3486470651	6.4481421347	-1.3749058941
H	-0.0755935615	8.7843373831	-2.0069812988
H	1.6137790203	10.5669597179	-1.5954784819
H	3.8231122482	11.0734045522	-0.8441459623
H	5.7930004609	12.0048100857	-0.0695131015
H	8.0490717199	11.6774258487	0.9061702618
H	8.8454340028	9.3759657350	1.4924239508
H	7.3869927891	7.4285634781	1.0633837455

Model 2

94

-2.4413357592346993e+03 frame 107   xyz file generated by TeraChem

C	2.8545067286	1.1886324328	0.3634188357
C	4.0071044885	0.5212294915	0.8222410485

C	3.9827873567	-0.8074549434	1.2399352813
C	2.7965420069	-1.5245474166	1.1124685311
C	1.5993538222	-0.9458440717	0.6400083726
C	1.6197947953	0.4606550459	0.3727463952
B	0.2938964670	-1.7455458988	0.4056658275
C	-0.9275288491	-0.9023502048	0.0630437257
C	-0.7878698585	0.4833238330	-0.2115302758
N	0.4126767178	1.1562292092	0.1370086478
C	-2.1824673616	-1.5261923590	-0.1571880457
C	-3.2307695652	-0.8248398222	-0.7717200310
C	-3.0172836737	0.4970992740	-1.1593632848
C	-1.8233672291	1.1625098109	-0.8790985830
C	0.0794285174	-3.2820929165	0.2705301549
C	-1.2551853189	-3.7725344823	0.1667732586
N	-2.3424031808	-2.8856617726	0.2038785673
C	1.1185035403	-4.2363581876	0.1963806545
C	0.8636636151	-5.6012405430	0.1264036015
C	-0.4540809060	-6.0554596773	0.0600549635
C	-1.5394232302	-5.1638957593	0.0126161155
C	-2.9370190837	-5.6180390511	-0.0915066837
C	-3.9104864537	-4.7428848925	0.4452499599
C	-3.5837674353	-3.3663393376	0.6900129125
C	-3.3580603913	-6.8874519466	-0.5980591169
C	-4.7002794658	-7.3455298603	-0.2991953892
C	-5.5819319620	-6.5219811159	0.4164603072
C	-5.2383697034	-5.2086165154	0.7620683982
C	-6.1454445898	-4.3250946805	1.4249968568
C	-5.7590090575	-3.0437865981	1.7361269361
C	-4.4812401754	-2.5528690396	1.3627741515
C	-2.5552124824	-7.7216121738	-1.4424892530
C	-3.0033460442	-8.9429557828	-1.8920214818
C	-4.2877691727	-9.4270523726	-1.5146818118

C	-5.1125964001	-8.6420363134	-0.7493506987
C	0.3638820120	2.5655110240	0.3673998920
C	1.5020195404	3.3530883175	0.0632315697
B	2.8570193474	2.6758655532	-0.0704556112
C	-0.7631711193	3.1651241267	0.9466579832
C	-0.7700593306	4.5479716758	1.1491943196
C	0.2868421235	5.3584189237	0.7403054492
C	1.4245520231	4.7649913382	0.1630199222
N	2.5289537154	5.5530748096	-0.2505812394
C	3.8286477852	5.0192336054	-0.3465208976
C	4.0506707509	3.6118135896	-0.3761235980
C	4.9241135292	5.9334932233	-0.4144440687
C	6.1899606610	5.4173743905	-0.7402840154
C	6.4049649676	4.0479120540	-0.9033405217
C	5.3553140267	3.1641452747	-0.6812497005
C	2.3210138652	6.8722738201	-0.7459220916
C	3.3908717802	7.8192119158	-0.6023330992
C	4.6821909513	7.3743643247	-0.2449160849
C	1.1349273176	7.2737861148	-1.3386834538
C	0.9209213013	8.6360248283	-1.6777743525
C	1.8703411324	9.5930700036	-1.4134753652
C	3.1353775634	9.2141218214	-0.8671612275
C	4.1552689674	10.1380641247	-0.6041259367
C	5.3811958155	9.7402747555	-0.0491575760
C	5.6622679699	8.3332633224	0.1541202422
C	6.3708062442	10.7085975377	0.3191018202
C	7.5509925708	10.3327948675	0.9099872708
C	7.8008959484	8.9573636824	1.1797902352
C	6.8916271349	7.9943581968	0.8063646552
H	4.9441936472	1.0767763250	0.8883029583
H	4.8807473999	-1.2831234293	1.6427134434
H	2.7829430725	-2.5684064742	1.4281121332

H	-4.1814811229	-1.3137103053	-0.9837530847
H	-3.8032281956	1.0256371152	-1.7061935575
H	-1.7017933518	2.1970238625	-1.1952771349
H	2.1545661425	-3.8982221632	0.1976998503
H	1.6879113151	-6.3190522454	0.1239784178
H	-0.6455347912	-7.1275447710	0.0525064108
H	-6.5718909250	-6.9024093636	0.6830101908
H	-7.1449952339	-4.6879141360	1.6775482636
H	-6.4446943900	-2.3748933893	2.2633646745
H	-4.2202179847	-1.5188828832	1.5869128610
H	-1.5865109483	-7.3581611084	-1.7837850906
H	-2.3744540426	-9.5385826384	-2.5593695933
H	-4.6234870488	-10.4081462296	-1.8611195055
H	-6.1172330128	-8.9840217923	-0.4848498815
H	-1.6174095031	2.5678785746	1.2634140730
H	-1.6278661061	5.0066847719	1.6489066626
H	0.2383349182	6.4340113480	0.9040077954
H	7.0158583022	6.1089499379	-0.9059910195
H	7.3925798200	3.6801011887	-1.1925463958
H	5.5328842480	2.0928734673	-0.7904513963
H	0.3379251315	6.5539529954	-1.5200117315
H	-0.0318803739	8.9179325210	-2.1341385889
H	1.6812467817	10.6481149257	-1.6274817415
H	3.9849135310	11.1967439618	-0.8192605728
H	6.1531551024	11.7648239596	0.1364144099
H	8.2886498171	11.0863554969	1.1986761583
H	8.7154831169	8.6654415797	1.7031729095
H	7.0893288722	6.9531697721	1.0606048310

Model 3

66

-1.7949498818125867e+03 frame 13   xyz file generated by TeraChem

C	0.9748689480	-1.7479906265	0.0194005474
C	1.7284138538	-2.9201326823	0.0113645111
C	0.9919043183	-4.1501362317	0.0505070013
C	-0.3992808126	-4.3049468499	0.0955862729
C	-1.1000306827	-3.0695956451	0.1017947752
C	-0.4330846907	-1.8405359562	0.0648905809
C	3.1631758422	-3.2844112034	-0.0287712398
C	3.1505341482	-4.6920881423	-0.0096742127
N	1.8835347846	-5.2111015678	0.0366484496
C	4.4538715305	-2.7259339719	-0.0765069253
C	5.6238182494	-3.5519247452	-0.1019794199
C	5.5245234240	-4.9539860044	-0.0802578338
C	4.2382718125	-5.5005962875	-0.0328779538
C	1.6065308510	-6.5571423802	0.0621601110
C	0.2265001727	-6.8848816272	0.1079002220
B	-0.8989480619	-5.7887258518	0.1285142952
C	-0.0643828424	-8.2735890600	0.1331290879
N	-1.4021119028	-8.5865412356	0.1779152051
C	-2.4860342622	-7.7231891498	0.2006244024
C	-2.3682308594	-6.3277254792	0.1792240046
C	-3.6955700308	-8.4923784349	0.2480745731
C	-4.8868327192	-7.7698757877	0.2756132399
C	-4.8316946362	-6.3594177946	0.2553202842
C	-3.6212435272	-5.6597832792	0.2089280568
C	2.6866758011	-7.5343547430	0.0406301145
C	2.2769043223	-8.8823144364	0.0692337007
C	0.9408957959	-9.3278712753	0.1154231609
C	-1.8869946262	-9.8674180268	0.2090591436
C	-3.2932427885	-9.9176282674	0.2538894496

C	-1.0499628804	-10.9335332038	0.1968359759
C	-1.5618632535	-12.2343937119	0.2298444889
C	-2.9602167903	-12.3711767384	0.2757319091
C	-3.8168524613	-11.2232653897	0.2876026940
B	4.1542763987	-7.0133136648	-0.0110784383
B	0.4594959117	-10.8094018436	0.1487492263
C	5.7069540052	-7.3779927277	-0.0551606651
C	6.4526024947	-6.1360066054	-0.0940499627
C	0.8650634411	-12.3527493219	0.1561935248
C	-0.3563193935	-13.1311787056	0.2036950094
C	2.0818000050	-13.0336276910	0.1275425196
C	2.1227191718	-14.4410946726	0.1440842415
C	0.9378719355	-15.1746734494	0.1893800981
C	-0.3094477752	-14.5208521056	0.2194796616
C	7.8424717567	-6.1465760349	-0.1372686829
C	8.5284032676	-7.3769272915	-0.1435014860
C	7.8264553110	-8.5810980779	-0.1067611413
C	6.4190384211	-8.5769823961	-0.0625830271
H	1.4568897793	-0.7670815293	-0.0086810925
H	-2.1913572799	-3.0650798382	0.1362641826
H	-1.0208022679	-0.9187406250	0.0712516498
H	4.5932255070	-1.6411820667	-0.0948933827
H	6.5956030984	-3.0509185132	-0.1384894663
H	-5.8541630373	-8.2780296090	0.3123063830
H	-5.7683540261	-5.7960719182	0.2768619648
H	-3.6547672686	-4.5684778837	0.1956436602
H	3.0609427581	-9.6460521934	0.0541992342
H	-3.4351941212	-13.3562661616	0.3034335023
H	-4.8970350112	-11.3916933028	0.3235363987

```
H    3.0215572226  -12.4736412404   0.0916249204
H    3.0856724850  -14.9591326394   0.1211629448
H    0.9746814739  -16.2677220383   0.2019043162
H   -1.2312129818  -15.1086957539   0.2549695139
H    8.4055932427   -5.2092947278  -0.1660238156
H    9.6215726483   -7.3851920014  -0.1775758279
H    8.3692217023   -9.5305834296  -0.1119155683
H    5.8838550044   -9.5313240403  -0.0340790630
```

References

1   M.-H. Tsai, Y.-H. Hong, C.-H. Chang, H.-C. Su, C.-C. Wu, A. Matoliukstyte, J. Simokaitiene, S. Grigalevicius, J. V Grazulevicius and C.-P. Hsu, , DOI:10.1002/adma.200600822.

2   O. Christiansen, H. Koch and P. Jørgensen, *Chem Phys Lett*, 1995, **243**, 409–418.

3   T. H. Dunning, *J Chem Phys*, 1989, **90**, 1007–1023.

4   M. J. Frisch, G. W. Trucks, H. B. Schlegel, G. E. Scuseria, M. A. Robb, J. R. Cheeseman, G. Scalmani, V. Barone, G. A. Petersson, H. Nakatsuji, X. Li, M. Caricato, A. Marenich, J. Bloino, B. G. Janesko, R. Gomperts, B. Mennucci, H. P. Hratchian, J. V. Ortiz, A. F. Izmaylov, J. L. Sonnenberg, D. Williams-Young, F. Ding, F. Lipparini, F. Egidi, J. Goings, B. Peng, A. Petrone, T. Henderson, D. Ranasinghe, V. G. Zakrzewski, J. Gao, N. Rega, G. Zheng, W. Liang, M. Hada, M. Ehara, K. Toyota, R. Fukuda, J. Hasegawa, M. Ishida, T. Nakajima, Y. Honda, O. Kitao, H. Nakai, T. Vreven, K. Throssell, Jr. J. A. Montgomery, J. E. Peralta, F. Ogliaro, M. Bearpark, J. J. Heyd, E. Brothers, K. N. Kudin, V. N. Staroverov, T. Keith, R. Kobayashi, J. Normand, K. Raghavachari, A. Rendell, J. C. Burant, S. S. Iyengar, J. Tomasi, M. Cossi, J. M. Millam, M. Klene, C. Adamo, R. Cammi, J. W. Ochterski, R. L. Martin, K. Morokuma, O. Farkas, J. B. Foresman and D. J. Fox, *Gaussian, Inc. Wallingford CT*.

5   F. Furche, R. Ahlrichs, C. Hättig, W. Klopper, M. Sierka and F. Weigend, *WIREs Computational Molecular Science*, 2014, **4**, 91–100.

6   C. Bannwarth, J. K. Yu, E. G. Hohenstein and T. J. Martínez, *J Chem Phys*, , DOI:10.1063/5.0003985.

7   I. S. Ufimtsev and T. J. Martinez, *J Chem Theory Comput*, 2009, **5**, 2619–2628.

8   X. Gao, S. Bai, D. Fazzi, T. Niehaus, M. Barbatti and W. Thiel, *J Chem Theory Comput*, 2017, **13**, 515–524.

9   Y. Niu, Q. Peng, C. Deng, X. Gao and Z. Shuai, *J Phys Chem A*, 2010, **114**, 7817–7831.

10   Y. Niu, W. Li, Q. Peng, H. Geng, Y. Yi, L. Wang, G. Nan, D. Wang and Z. Shuai, *Mol Phys*, 2018, **116**, 1078–1090.

11   Lindahl, Abraham, Hess and van der Spoel, , DOI:10.5281/ZENODO.4723561.

12   B. Hess, H. Bekker, H. J. C. Berendsen and J. G. E. M. Fraaije, *J Comput Chem*, 1997, **18**, 1463–1472.

13   W. F. Van Gunsteren and H. J. C. Berendsen, *Mol Simul*, 1988, **1**, 173–185.

14   M. Parrinello and A. Rahman, *J Appl Phys*, 1981, **52**, 7182–7190.

15   Y.-C. Cheng, X.-C. Fan, F. Huang, X. Xiong, J. Yu, K. Wang, C.-S. Lee and X.-H. Zhang, , DOI:10.1002/anie.202212575.

16   T. Hua, L. Zhan, N. Li, Z. Huang, X. Cao, Z. Xiao, S. Gong, C. Zhou, C. Zhong and C. Yang, *Chemical Engineering Journal*, , DOI:10.1016/J.CEJ.2021.131169.

17   X. Wu, B. K. Su, D. G. Chen, D. Liu, C. C. Wu, Z. X. Huang, T. C. Lin, C. H. Wu, M. Zhu, E. Y. Li, W. Y. Hung, W. Zhu and P. T. Chou, *Nature Photonics 2021 15:10*, 2021, **15**, 780–786.